The sHSP22 Heat Shock Protein Requires the ABI1 Protein Phosphatase to Modulate Polar Auxin Transport and Downstream Responses[1][OPEN]

Yanli Li,[a,b,2] Yaqiong Li,[a,b,2] Yongchang Liu,[c] Yaorong Wu,[a,3] and Qi Xie[a,b,3]

[a]State Key Laboratory of Plant Genomics, Institute of Genetics and Developmental Biology, Chinese Academy of Sciences, Beijing 100101, China

[b]University of Chinese Academy of Sciences, Beijing 100049, China

[c]College of Chemistry and Bioengineering, Hunan University of Science and Engineering, Yongzhou, Hunan 425199, China

ORCID IDs: 0000-0002-4318-9099 (Y.L.L.); 0000-0002-4752-6275 (Y.R.W.); 0000-0002-8262-9093 (Q.X.).

The phytohormones abscisic acid (ABA) and indole-3-acetic acid (IAA) response pathways interact synergistically or antagonistically to regulate plant development and environmental adaptation. Here, we show that *ABI1*, a key negative regulator of ABA signaling, is essential for auxin-modulated root development. We performed a microarray analysis using the loss-of-function mutant *abi1-3* and Col-0 seedlings treated with IAA. For *sHSP22*, an endoplasmic reticulum (ER) small heat shock protein-encoding gene, the induction by IAA was dependent on *ABI1*. *shsp22* displayed enhanced sensitivity to ABA in primary root growth. In contrast, overexpression of full-length, but not truncated sHSP22 lacking signal peptide and ER-retention sequences, resulted in decreased ABA sensitivity. Overexpressed (OX) *sHSP22* partially rescued the ABA hypersensitivity of *abi1-3*. In addition, *sHSP22* is involved in auxin-regulated hypocotyl elongation at high temperature treatment. *sHSP22* also affected accumulation of auxin efflux carrier PIN proteins due to potentiated intracellular trafficking. And *sHSP22 OX* lines initiated more lateral roots after auxin application. Our results suggest that sHSP22 regulates auxin response through modulating auxin polar transport, and ABI1-sHSP22 provides a novel module orchestrating ABA and auxin signaling crosstalk in Arabidopsis (*Arabidopsis thaliana*).

Plants exhibit tremendous plasticity and adaptability in growth and development to coordinate with environmental conditions. Phytohormone levels and signaling are fine-tuned to execute central roles in perceiving and initiating appropriate responses. Mounting evidence supports the hypothesis that plant hormones act in the context of large regulatory networks affecting each other's synthesis and response pathways (Kuppusamy et al., 2009). Among these hormones, indole-3-acetic acid (IAA) and abscisic acid (ABA) interplay dynamically in diverse physiological processes (Vanstraelen and Benková, 2012).

IAA, the most abundant endogenous auxin, is the best-characterized hormone affecting morphogenesis and tropisms in Arabidopsis (*Arabidopsis thaliana*). Spatiotemporal asymmetric auxin distribution patterns within different tissues direct such developmental processing (Vanneste and Friml, 2009; Sauer et al., 2013). Auxin metabolism, including biosynthesis, conjugation, and cellular transport, determines its distribution pattern (Ikeda et al., 2009; Zhao, 2010). The polar auxin transport facilitators, such as membrane-localized ATAUX1/LIKE AUX1 (AUX1/LAX) influx transporters and ATP-BINDING CASSETTE B (ABCB), PIN-FORMED (PIN) protein efflux carriers, transport auxin in a cell-to-cell manner to establish the auxin gradients that is essential for organogenesis (Bennett et al., 1996; Benková et al., 2003; Swarup et al., 2008). Auxin accumulation within an individual cell is interpreted by a short nuclear-localized signaling pathway to induce transcriptional responses. Auxin binds to the F-box protein TIR1/AFB, a subunit of ubiquitin E3 ligase $SCF^{TIR1\text{-}AFBs}$ (Skp1-cullin-F box protein), in the presence of Aux/IAA repressor proteins, thus mediating Aux/IAA ubiquitylation and degradation by the 26S proteasome, consequently releasing ARF (AUXIN RESPONSE FACTOR) transcriptional activity (Gray et al., 2001; Dharmasiri et al., 2005; Kepinski and Leyser, 2005). The auxin sensitive reporters *DR5:GUS* (Ulmasov et al., 1997) and *DR5:GFP*

[1] This research was supported by National Key R&D Program of China grants 2016YFA0500500 and 2015CB942900 and by National Natural Science Foundation of China grants 31571441 and 91317308.

[2] These authors contributed equally to the article.

[3] Address correspondence to qxie@genetics.ac.cn or yrwu@genetics.ac.cn.

The authors responsible for distribution of materials integral to the findings presented in this article in accordance with the policy described in the Instructions for Authors (www.plantphysiol.org) are: Qi Xie (qxie@genetics.ac.cn) and Yaorong Wu (yrwu@genetics.ac.cn).

Q.X. and Y.R.W. conceived this project and designed all research with help from Y.L.L.; Y.L.L. and Y.Q.L. performed the experiments and analyzed the data with assistance from Y.C.L. under the supervision of Q.X. and Y.R.W.; Q.X., Y.R.W., and Y.L.L. wrote the article.

[OPEN] Articles can be viewed without a subscription.

www.plantphysiol.org/cgi/doi/10.1104/pp.17.01206

(Friml et al., 2003) are extensively utilized to monitor auxin responses.

ABA regulates many aspects of plant growth and development, such as seed maturation and dormancy, root growth maintenance, vegetative development, and reproduction. In addition, ABA functions as a "stress hormone" that perceives and reacts to environmental challenges such as drought, salinity, heat, and cold (Zhu, 2002). The underlying mechanism relies on reprogramming the transcription of stress-responsive protective genes and regulatory signaling components (Shinozaki and Yamaguchi-Shinozaki, 2007). Elucidation of ABA signaling transduction pathway highlights type 2C protein phosphatases such as ABI1, which act as important upstream negative regulators. The second messengers, phosphatidic acid and hydrogen peroxide, both decrease the phosphatase activity of ABI1 (Meinhard and Grill, 2001; Zhang et al., 2004), emphasizing ABI1 as a hub that integrates second messenger signaling and different effectors mediated stress tolerance (Cutler et al., 2010).

Previous research shows that auxin and ABA have complex and extensive cross-talk in seed germination, seedling establishment, and lateral root emergence. The auxin reporter, *DR5:GUS*, exhibits asymmetric expression that is maximal at the meristems during Arabidopsis seed germination, which suggests that an auxin gradient is essential for early seedling meristem establishment and maintenance (Tanaka et al., 2006). ABA represses postgermination axis elongation through combinatorial modulation of auxin transport facilitators AUX1 and PIN2, and down-regulation of AXR2/IAA7-mediated signal transduction (Belin et al., 2009). Additionally, ARF10 repression by *MIR160* has been proven to be important for seed germination and postembryonic development (Liu et al., 2007). ARF2 modulates ABA response in Arabidopsis by down-regulating the expression of homeodomain gene *HB33* (Wang et al., 2011). DEXH box RNA helicase is involved in the crosstalk between ABA and auxin signaling by mediating mitochondrial reactive oxygen species production in Arabidopsis (He et al., 2012). All these findings demonstrate that ABA and auxin counteract each other at these phases of development.

Both ABA and auxin are involved in lateral root development. The *ABA-insensitive 8* mutant displays limited lateral roots due to a defect in root meristem activity (Brocard-Gifford et al., 2004). *Lateral root development 2* plays an essential role in repressing lateral root development under osmotic stress, and likely influences lateral root development by interfering with auxin signaling (Deak and Malamy, 2005). Moreover, ABI3 modulated by farnesylation acts as an interaction node that involves auxin signaling and is required for lateral root formation (Brady et al., 2003). The transcription factor *WRKY46* acts upstream of *ABI4* to promote lateral root initiation under osmotic/salt conditions via regulation of auxin homeostasis (Ding et al., 2015). Additionally, *ibr5*, mutant of *IBR5* encoding dual-specificity phosphatase, shows the decreased sensitivity to both ABA and auxin. Further research discovers that IBR5 interacts with and dephosphorylates MPK12 to regulate auxin signaling; nevertheless, how *ibr5* responds to ABA remains to be determined (Monroe-Augustus et al., 2003; Strader et al., 2008; Lee et al., 2009). Moreover, auxin signaling mutants *axr1*, *axr2/iaa7*, *slr/iaa14*, *iaa16*, and *axr3/iaa17* all differentially respond to applied ABA compared with wild-type plants, suggesting that Aux/IAA-dependent auxin signaling also affects ABA activity (Fukaki et al., 2002; Tiryaki and Staswick, 2002; Rinaldi et al., 2012). Despite description of multiple genes mediating ABA and auxin crosstalk, the fundamental mechanisms underlying their interconnection remain rudimentary.

Small heat shock proteins (sHSPs) are ubiquitously distributed and comprise a family of proteins that are characterized by a conserved α-crystallin domain and range in size from 15 to 45 kD (Jakob et al., 1993; Basha et al., 2006). The representative α-crystallin domain contains a beta sandwich composed of about 90 amino acid residues, which is flanked by a variable N-terminal and a short C-terminal extension (MacRae, 2000). sHSP expression is induced under heat shock conditions as well as under other abiotic and biotic stresses. A number of sHSPs are involved in plant development such as seed maturation and germination, embryogenesis, as well as pollen development (Waters et al., 1996). Crystal structures of an archaea HSP16.5 from *Methanococcus jannaschii* and a plant HSP16.9 from wheat (*Triticum aestivum*) revealed large oligomers and the architectural basis for molecular chaperone activity (Kim et al., 1998; van Montfort et al., 2001). sHSP complexes bind and prevent irreversible denatured aggregation in an ATP-independent manner, thereby conferring thermotolerance to heat shock (Haslbeck et al., 2005). While a limited number of orthologs exist in other organisms, Arabidopsis has a relatively large family of 19 sHSPs that are classified into cytosolic, chloroplastic, endoplasmic reticulum (ER), and mitochondrial members based on their subcellular localization (Scharf et al., 2001). Although no clear explanation accounts for the exact molecular function of plant sHSPs in addition to heat acclimation, recent studies have shed light on sHSP's role in protein translocation, lipid interaction, and maintenance of membrane integrity (Török et al., 2001; Chowdary et al., 2007; Balogi et al., 2008; Kim et al., 2011).

Distinct from other Arabidopsis sHSPs, sHSP22 is the only identified sHSP localized in ER with a specific signal peptide and the ER retention tetrapeptide SKEL, which shares 64.5% amino acid similarity to class I cytosolic sHSP17.6 (Helm et al., 1995). However, the molecular and physiological function of sHSP22 remains to be elucidated.

In this study, we show that a loss-of-function allele in *ABI1*, a significant negative regulator of ABA signal transduction, exhibits decreased sensitivity to exogenous auxin in lateral root formation. In search of downstream targets of ABI1 essential for auxin-involved lateral root development, microarray analysis

highlights ABI-dependent *sHSP22* expression. Further genetic and physiological examination of *sHSP22* loss-of-function and overexpression plants demonstrates that ER-localized *sHSP22* negatively regulates ABA signaling, whereas overexpression of *sHSP22* enhances auxin-associated hypocotyl elongation at high temperature and increases sensitivity in root growth to auxin transport inhibitor naphthyl phthalamic acid (NPA). *sHSP22* affects intracellular vesicle trafficking of PIN proteins. As a consequence, overexpression of *sHSP22* promotes increased lateral root number when seedlings were treated by auxin.

RESULTS

ABI1 Is Involved in Auxin-Triggered Lateral Root Development

Exogenous auxin application can promote lateral root development (Benková et al., 2003), which has been widely employed to identify mutants with altered auxin responses. To identify more players in crosstalk between ABA and auxin signal transduction pathways, we screened major ABA signaling mutants for changes in lateral root formation of auxin application, including natural IAA and a synthetic analog1-napthalene acetic acid (NAA). We show that *abi1-3*, a loss-of-function allele of *ABI1* that is hypersensitive to ABA in germination (Saez et al., 2006), decreased sensitivity to exogenous auxin compared with Col-0 (Fig. 1A). Although treatment of Col-0 plants with 100 nM NAA or 100 nM IAA resulted in 10-fold and 4-fold more lateral roots, respectively, a reduction in lateral root number was observed in *abi1-3* (Fig. 1, A and B). In support, another two *abi1* mutants were also tested. As shown in Supplemental Figure S1, the knockdown mutant *abi1-2* displayed similar phenotype with *abi1-3*, whereas *abi1-11*, a gain-of-function *abi1-1* analog in Col ecotype, has no dramatic difference from wild type. The lower sensitivity of *abi1* to auxin treatment in lateral root development suggested that *ABI1* is required for auxin-stimulated lateral root development. Given that ABI1 operates as a key repressor in the ABA signaling pathway, we supposed that it plays a role in the interconnection between ABA and auxin.

sHSP22 Expression Induced by IAA Treatment Is Dependent on *ABI1*

To explore the function of *ABI1* in response to IAA treatment, we performed a microarray analysis using RNA prepared from *abi1-3* and Col-0 seedlings treated with or without IAA for a time course of 0, 2, and 6 h. From the differential expressed genes of the microarray data (Supplemental Table S1), we searched for genes whose transcripts were induced by IAA in Col-0, but were attenuated or absent in *abi1-3*. We identified *sHSP22* encoding a sHSP. No function of this gene was reported. We further analyzed in detail its function in plant response to IAA and ABA treatments. As shown

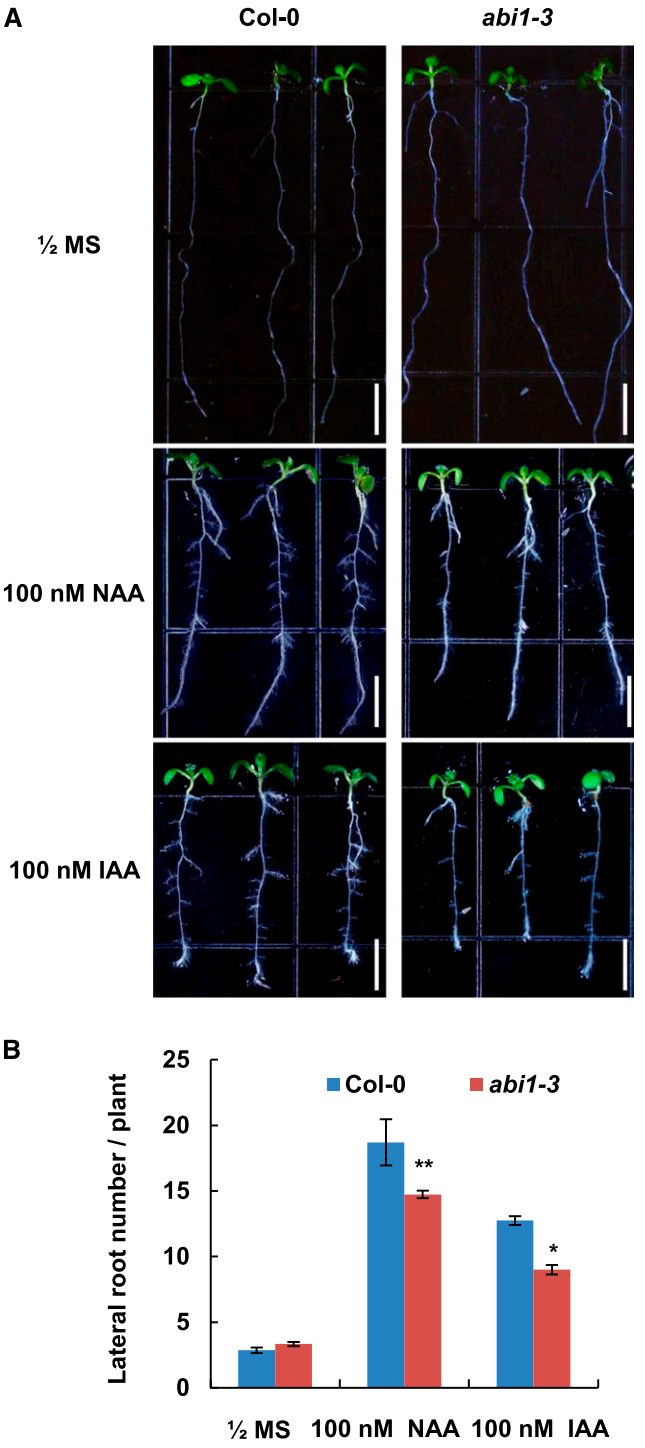

Figure 1. Lateral root development of *abi1-3* decreases sensitivity to exogenous auxin. A, Five-day-old Col-0 and *abi1-3* seedlings were transferred to half-strength MS medium supplemented with 0 and 100 nM IAA and 100 nM NAA and grown for additional 3 d. Bar = 0.5 cm. B, Statistics assay of lateral root number of Col-0 and *abi1-3* seedlings shown in A. The error bars represent ±SD for one biological replicate (n = 30); three biological experiments were performed. $^{**}P < 0.01$ and $^{*}P < 0.05$.

A

Treatment	*sHSP22* expression	
IAA, 0 hr	Col-0	210
	abi1-3	643
IAA, 2 hr	Col-0	6432
	abi1-3	656
IAA, 6 hr	Col-0	205
	abi1-3	344

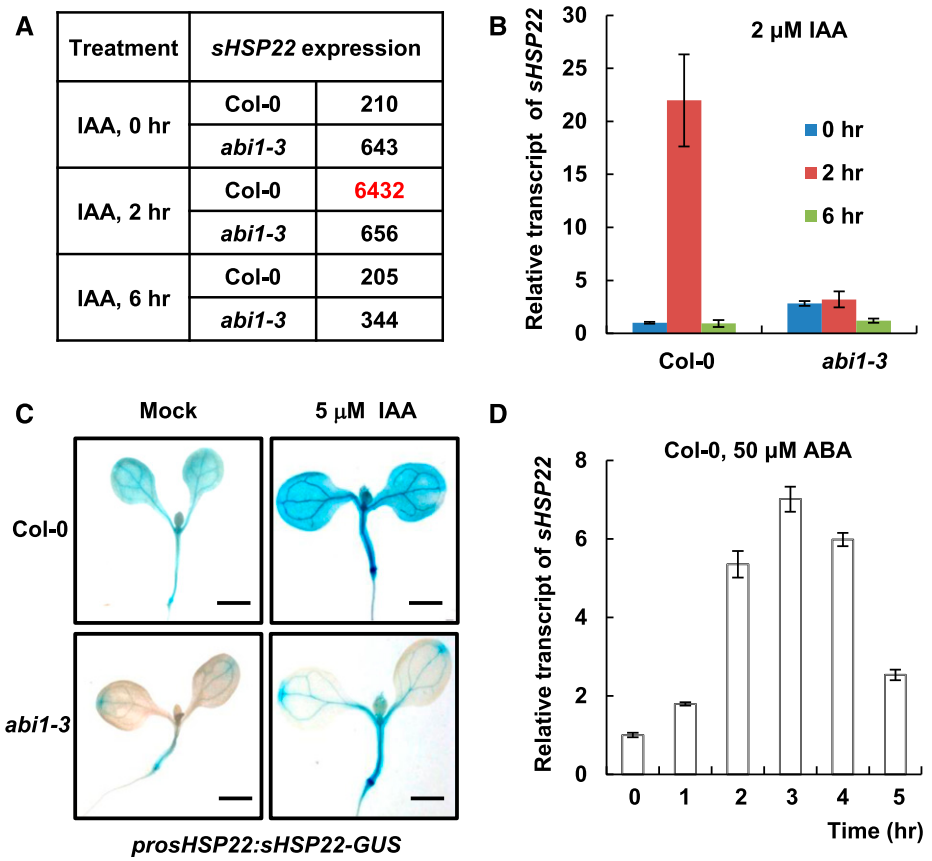

Figure 2. Expression of *sHSP22* induced by IAA is dependent on ABI1. A, Microarray data for *sHSP22* expression in 2-week-old wild-type and *abi1-3* seedlings treated with 2 μM IAA for a time course of 0, 2, and 6 h. B, Confirmation of *sHSP22* expression in A using qRT-PCR. C, Analysis of *prosHSP22:sHSP22-GUS* expression in the wild type and *abi1-3*. Five-day-old Col-0 and *abi1-3* seedlings were treated with half-strength MS liquid supplemented with 0 or 5 μM IAA for 6 h and subjected to GUS staining. Bar = 2 mm. D, Expression of *sHSP22* in response to 50 μM ABA treatment. Two-week-old Col-0 seedlings were treated with ABA for the time course of 0, 1, 2, 3, 4, and 5 h and harvested for RNA extraction and qRT-PCR. For B and D, *sHSP22* transcript levels were normalized to *ACTIN2* expression, and error bars represent ±SD of triplicates.

in Figure 2A, *sHSP22* was strongly and transiently induced at 2 h of IAA treatment in Col-0, whereas this induction was completely absent in *abi1-3*. Subsequent qRT-PCR confirmed the microarray results (Fig. 2B), suggesting that IAA rapidly activated *ABI1*-dependent expression of *sHSP22*. Because there is an adjacent gene mutation of *MAP Kinase Kinase 1* (*MKK1*) in *abi1-3* (Wu et al., 2015), we detected the expression levels of *sHSP22* in the relevant materials to rule out the possibility that *sHSP22* was influenced by *MKK1*. The result showed that the expression levels of *sHSP22* are not affected by the additional mutation of *MKK1* in *abi1-3* (Supplemental Fig. S2). Moreover, we introduced sHSP22 fused with GUS reporter driven by its native promoter into Col-0 and *abi1-3*. Histochemical staining of 5-d-old Col-0 seedlings revealed that sHSP22-GUS was expressed in vasculature tissue of leaf, hypocotyl, and root, and enhanced in presence of 5 μM IAA. Conversely, expression of sHSP22-GUS decreased in *abi1-3* and increased much less upon IAA treatment compared with Col-0 seedlings (Fig. 2C). The auxin-enhanced *sHSP22* transcription was also observed in roots (Supplemental Fig. S3, A and B), and the sHSP22 distribution in the vasculature implicates a specific function during auxin response. In addition, we also investigated the expression of *sHSP22* when seedlings were treated by ABA in a time course. The transcript of *sHSP22* was enhanced at 1 h, reached a maximum after 3 h, and then decreased (Fig. 2D). The ABA-induced *sHSP22* transcription was also observed in roots (Supplemental Fig. S3C), indicating that *sHSP22* was also regulated by ABA.

shsp22 Exhibits Enhanced Sensitivity to ABA

To elucidate the function of *sHSP22* in ABA signaling, we employed a reverse genetics approach. One transposon insertion mutant from the Riken Bioresource Center (Ito et al., 2002; Kuromori et al., 2004), Ds13-4798-1, was identified and designated as *shsp22-1*. The transposon was inserted into the only exon of *sHSP22* +288 and +361 relative to translation start (Fig. 3A). A homozygous mutant was verified through diagnostic PCR using *sHSP22*-specific and T-DNA border primers (Fig. 3B), and further transcript validation through RT-PCR showed that *shsp22* is a null allele (Fig. 3C). Then we examined the *shsp22* response to ABA in root growth compared with its wild-type Nossen (No-0) ecotype. When grown in an ABA-free medium, no distinct differences were observed between *shsp22* and No-0. However, in the presence of a concentration gradient of 0.5, 1.0, and 1.5 μM ABA, *shsp22* exhibited enhanced sensitivity to primary root growth inhibition in a dose-dependent manner (Fig. 3, D and E).

Because only one insertion line was identified, we also introduced *sHSP22* under control of its own

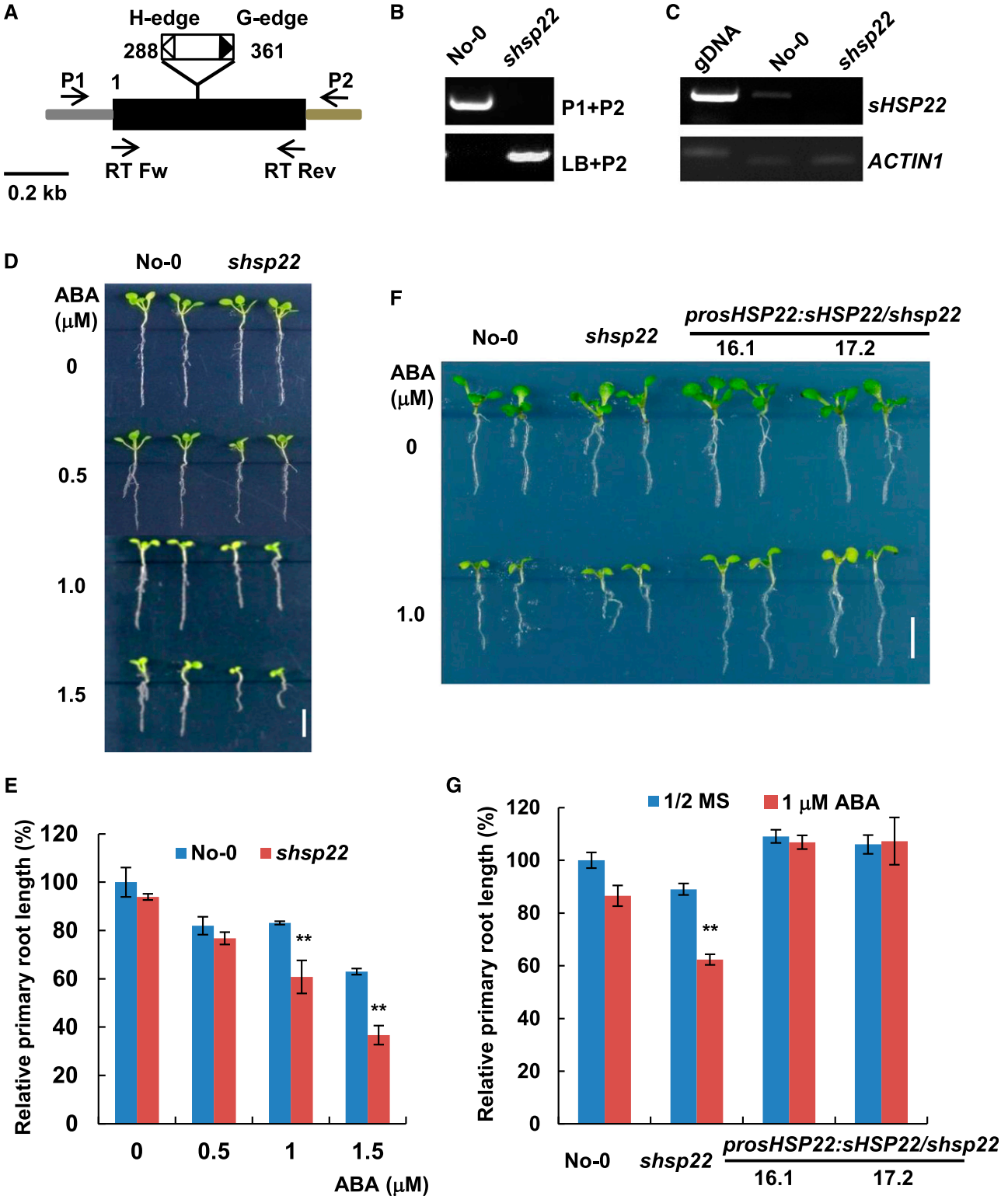

Figure 3. *shsp22* exhibits enhanced sensitivity to ABA. A, Schematic representation of the Ds transposon insertion *shsp22* mutant. The black box indicates the coding region, and the gray and brown bar indicates the 5′-and 3′-untranslated regions, respectively. The white and black triangles show the H-edge and G-edge of the Ds transposon, respectively. The numbers indicate the transposon insertion position. P1, forward primer; P2, reverse primer; LB, primer specific to the Ds transposon G edge. RT Fw and RT Rev were primers used for RT-PCR analysis. B, Diagnostic PCR of the Ds transposon inserted *sHSP22*. DNA from the homozygous insertion line of *shsp22* was used. Primers used for PCR are indicated on the right of each lane. C, RT-PCR analysis of

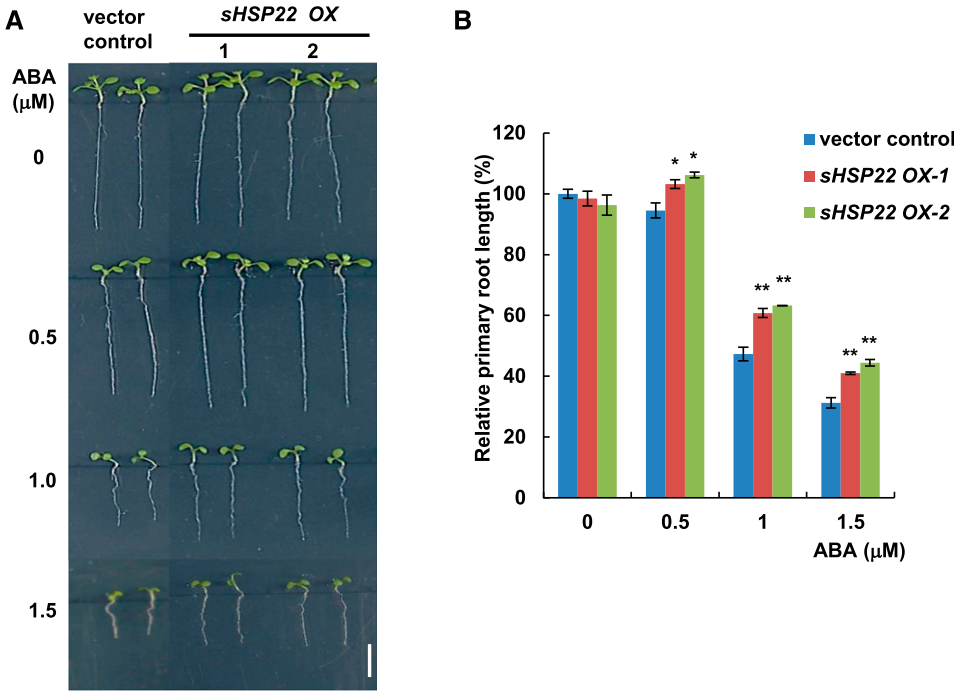

Figure 4. Overexpression of *sHSP22* confers reduced sensitivity to ABA. A, Root phenotype of *sHSP22* overexpression seedlings and vector control grown horizontally on half-strength MS medium with or without various ABA concentrations (0, 0.5, 1.0, and 1.5 μM). Representative seedlings were shown after 9 d of growth. Bar = 0.5 cm. B, Statistics assay of relative primary root length of seedlings shown in A. Error bars represent ±SD of one biological replicate (n = 30); three biological experiments were performed. $^{**}P < 0.01$ and $^{*}P < 0.05$.

promoter into *shsp22* mutant, and transgenic lines with a transcript abundance comparable to No-0 as demonstrated through qRT-PCR (Supplemental Fig. S4) could fully complement *shsp22* increased sensitivity phenotype to ABA during primary root growth (Fig. 3, F and G). Therefore, the results reinforced the notion that elevated ABA sensitivity in *shsp22* is due to *sHSP22* dysfunction.

sHSP22 Overexpression Plants Are Less Sensitive to ABA

To further address the role of *sHSP22* in ABA response, we examined phenotypes of *sHSP22* overexpression plants. Expression of *myc-sHSP22* driven by CaMV 35S promoter was introduced into Col-0 Arabidopsis. T3 homozygous *sHSP22 OX* lines were obtained, and transcript levels and protein accumulation in 2-week-old seedlings were evaluated by northern blot and western blot, respectively (Supplemental Fig. S5, A and B). Compared with Col-0 and empty vector control, significant increases in transcripts of *sHSP22* and Myc-fused protein were observed in *sHSP22 OX* plants. We chose one empty vector control (line 5.6) and two *sHSP22 OX* lines (1.2, 4.5, designated as *sHSP22 OX-1* and *sHSP22 OX -2*, respectively) for the subsequent phenotypic analysis.

sHSP22 OX lines were less sensitive to the inhibition of primary root growth caused by ABA (Fig. 4, A and B). In addition, transplanting 5-d-old seedlings from ABA-free to medium supplemented with 0, 15, and 30 μM ABA confirmed that *sHSP22 OX* lines were less sensitive to ABA during primary root growth (Supplemental Fig. S6, A and B). Collectively, the opposite phenotypes of *sHSP22 OX* to *shsp22* demonstrated that *sHSP22* confers negative effects on ABA signaling.

sHSP22 Is Located in the ER and the Localization Is Important for Its Biological Function

sHSP22 was first identified from Arabidopsis as an ortholog to the endomembrane protein PsHSP22.7 (Helm et al., 1993) with 70% identity and 87% similarity

Figure 3. (*Continued.*)
the *sHSP22* transcripts in the wild-type and Ds transposon insertion mutant seedlings. The primer pairs used for RT-PCR are shown in A. *ACTIN1* was used as an internal control. D, Primary root growth of the wild type and *shsp22* on half-strength MS medium containing a range of ABA concentrations (0, 0.5, 1.0, and 1.5 μM). The seeds were germinated for 8 d in half-strength MS medium with or without ABA, and representative plants are shown. Bar = 0.5 cm. E, Statistics assay of relative primary root length in No-0 and *shsp22* seedlings shown in D. Error bars represent ±SD of one biological replicate (n = 30); three biological experiments were performed. $^{**}P < 0.01$. F, Root phenotypes of No-0, *shsp22*, and *shsp22* complementation seedlings grown horizontally in half-strength MS medium with or without 1.0 μM ABA. Representative seedlings were shown after 9 d of growth. Bar = 0.5 cm. G, Statistics assay of relative primary root length in seedlings as shown in F. Error bars represent ±SD of one biological replicate (n = 30); three biological experiments were performed. $^{**}P < 0.01$.

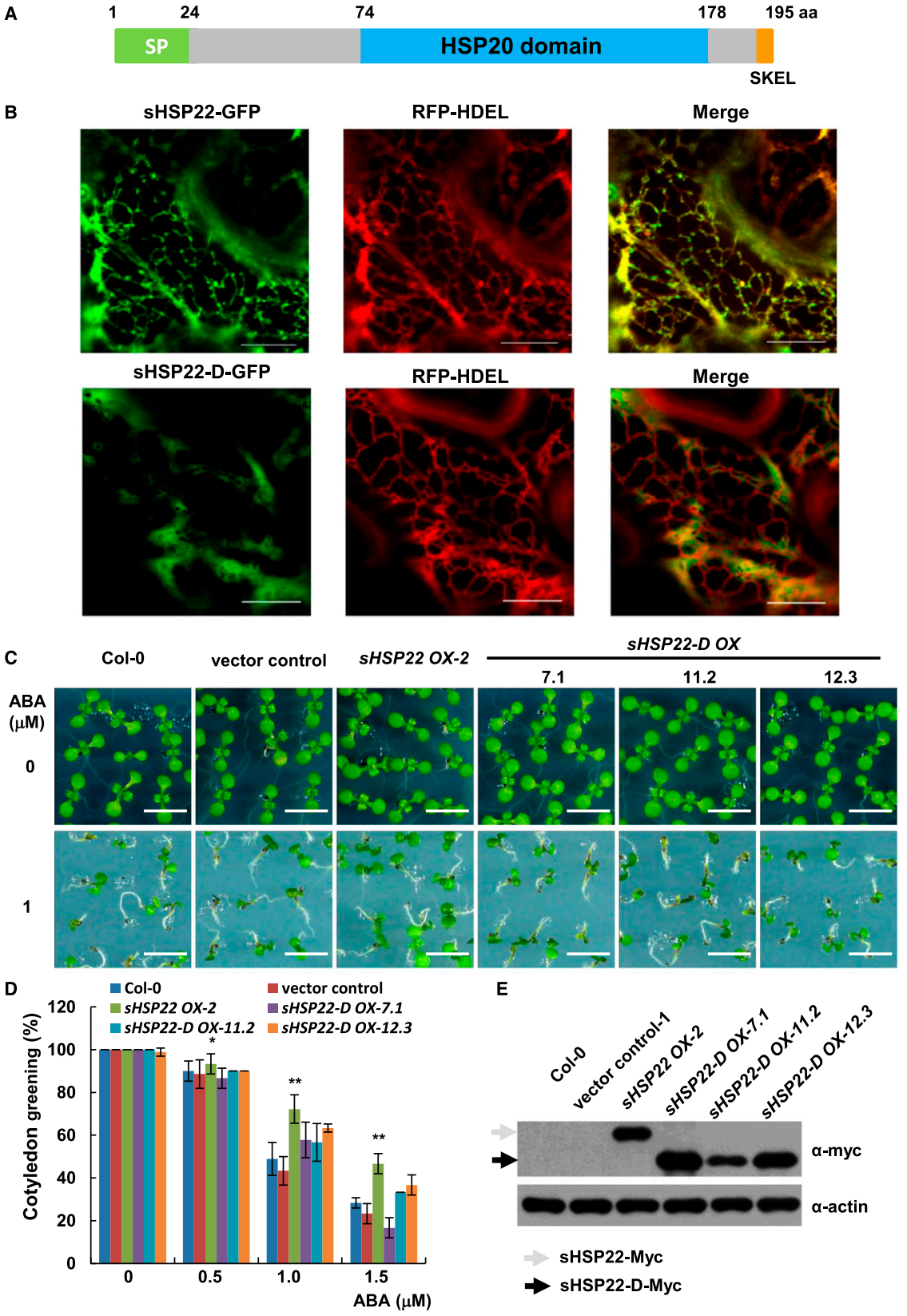

Figure 5. ER localization of sHSP22 contributes to ABA response. A, Schematic diagram of the sHSP22 structure. Representative parts of signal peptide, HSP domain, and ER retention tetrapeptide are shown in green, light-blue, and orange boxes, respectively.

in amino acid sequence; hence, it was thought to be the only small endomembrane localization heat shock protein in Arabidopsis (Helm et al., 1995). However, its subcellular localization and physiological function remained unclear. First, sHSP22 was aligned with the following orthologs: sHSP22 has 49% amino acid similarity with HSP26p from yeast and 49%, 51%, and 41% similarity to human α-crystallin A chain (HSPB4), heat shock protein β1 (HSPB1), and heat shock protein β3 (HSPB3), respectively. The alignment revealed that they share a conserved α-crystallin domain composed of 2 hydrophilic subdomains essential for oligomer assembly in addition to divergent N terminus and variable C-terminal extensions (Supplemental Fig. S7A). Next, sHSP22 structure predicted by SMART web service includes a predicted N-terminal signal peptide, a characteristic HSP20 domain, and a putative C-terminal tetrapeptide for ER retention (Fig. 5A). Particularly, phylogenetic trees based on amino acid sequence similarity in Arabidopsis showed that ER-localized sHSP22 most resembled class I cytosolic sHSP17.6, 18.1, and 17.4 (Supplemental Fig. S7B). Transient expression of sHSP22-GFP and the ER-localized marker red florescent protein (RFP)-HDEL by coagroinfiltration in *Nicotiana benthamiana* (Liu et al., 2010) showed that their fluorescent images were largely coincident with at least the ER localization pattern. However, the truncated sHSP22-D-GFP, in which the signal peptide and the ER retention tetrapeptide deleted from coding sequence of *sHSP22*, abolished the typical ER localization and partially localized in nucleus (Fig. 5B; Supplemental Fig. S7C). These are direct evidence for ER localization of sHSP22.

We speculated that the specific ER localization confers to sHSP22 unique functions distinct from other cytosolic sHSPs. To confirm this hypothesis, we generated the Myc-fused *sHSP22-D* transgenic plants and confirmed myc-fused protein levels using anti-myc antibody in three independent homozygous lines (Fig. 5E). Subsequent examination of *sHSP22-D OX* response to ABA showed that, despite reduced sensitivity of *sHSP22 OX*, the truncated *sHSP22-D OX* plants showed similar phenotypes to Col-0 and vector control in presence of a concentration gradient of 0.5, 1.0, and 1.5 μM ABA. Both the relative primary root length and cotyledon greening percentage confirmed this tendency (Fig. 5, C and D; Supplemental Fig. S8). These data indicate that proper ER localization of sHSP22 is important for plant to response to ABA.

Overexpression of *sHSP22* Partially Rescued *abi1-3* Hypersensitivity to ABA

To dissect the relationship between *ABI1* and *sHSP22*, we constitutively expressed *sHSP22-myc* under control of the *35S* promoter in the ABA-hypersensitive mutant *abi1-3* and investigated the corresponding phenotype to ABA (Fig. 6). Compared with wild type and *abi1-3*, elevated transcript levels of *sHSP22* in *abi1-3/sHSP22* homozygous lines were demonstrated using real-time PCR (Supplemental Fig. S9). When grown in medium containing 0.5 or 1.0 μM ABA, *abi1-3* exhibited the same hypersensitive phenotype as reported by Saez et al. (Saez et al., 2006); however, the *abi1-3/sHSP22* complement lines partially rescued *abi1-3* hypersensitivity to ABA in both post-germination cotyledon greening and primary root growth (Fig. 6, A–C).

sHSP22 Promotes Hypocotyl Elongation at High Temperature

Because the *ABI1*-dependent transcription of *sHSP22* was greatly induced by auxin (Fig. 2, B and C), we investigated whether sHSP22 correlated with ABI1 to respond to auxin. Auxin promotes hypocotyl elongation, a response that can be monitored when Arabidopsis seedlings are grown at 29°C (Gray et al., 1998). Because expression of *sHSP22* is dramatically induced under heat shock conditions (Winter et al., 2007) and the high temperature-induced *sHSP22* transcription was also observed in hypocotyls (Supplemental Fig. S3D), hypocotyl elongation of *shsp22* and *sHSP22 OX* lines under such conditions was examined. At 22°C, *shsp22* and No-0 grew similar short hypocotyls, approximately 2 mm. At 29°C, hypocotyls of both genotypes were prolonged, but *shsp22* developed reduced length of hypocotyls by 18% compared with No-0 (Fig. 7, A and B). In contrast, hypocotyl elongation of 6-d-old *sHSP22 OX-2* seedlings was clearly enhanced by 58% at 29°C compared with Col-0 (Fig. 7, C and D), which suggests an enhanced auxin response. Previous research demonstrated that Arabidopsis hypocotyl elongation at high temperature resulted from cell expansion, which was promoted by a number of factors, such as auxin biosynthesis involving phytochrome-interacting factor 4 (PIF4; Franklin et al., 2011; Sun et al., 2012), auxin signaling, and auxin transport. When grown on medium supplemented with

Figure 5. (*Continued.*)
B, Colocalization of sHSP22-GFP (top) and sHSP22-D-GFP (bottom) with RFP-HDEL. RFP-HDEL is an ER localization peptide motif fused with RFP. Tobacco leaves were infiltrated with agrobacteria bearing *35S:sHSP22-GFP* and *35S:RFP-HDEL* or *35S:sHSP22-D-GFP* and *35S:RFP-HDEL* constructs. After 3 d, tobacco leaves were cut and simultaneously subjected to confocal microscopy observation. C, Cotyledon greening phenotype of Col-0, vector control, *sHSP22 OX-2*, and *sHSP22-D* overexpression plants. Representative seedlings were sown 9 d after imbibition on 1 μM ABA. Bar = 0.5 cm. D, Statistical analysis of different genotype plants shown in C. The cotyledon greening percentage was calculated after the 9-d growth in the medium. The error bars represent ±SD (triplicate measurements; $n = 90$). The asterisks indicate a significant difference between *sHSP22* overexpression and control plants (**$P < 0.01$ and *$P < 0.05$). E, sHSP22-D accumulation in overexpressing and control plants by western blotting using anti-myc antibody. The gray and black arrows separately denote whole and truncated sHSP22 protein form respectively. Actin is used as control.

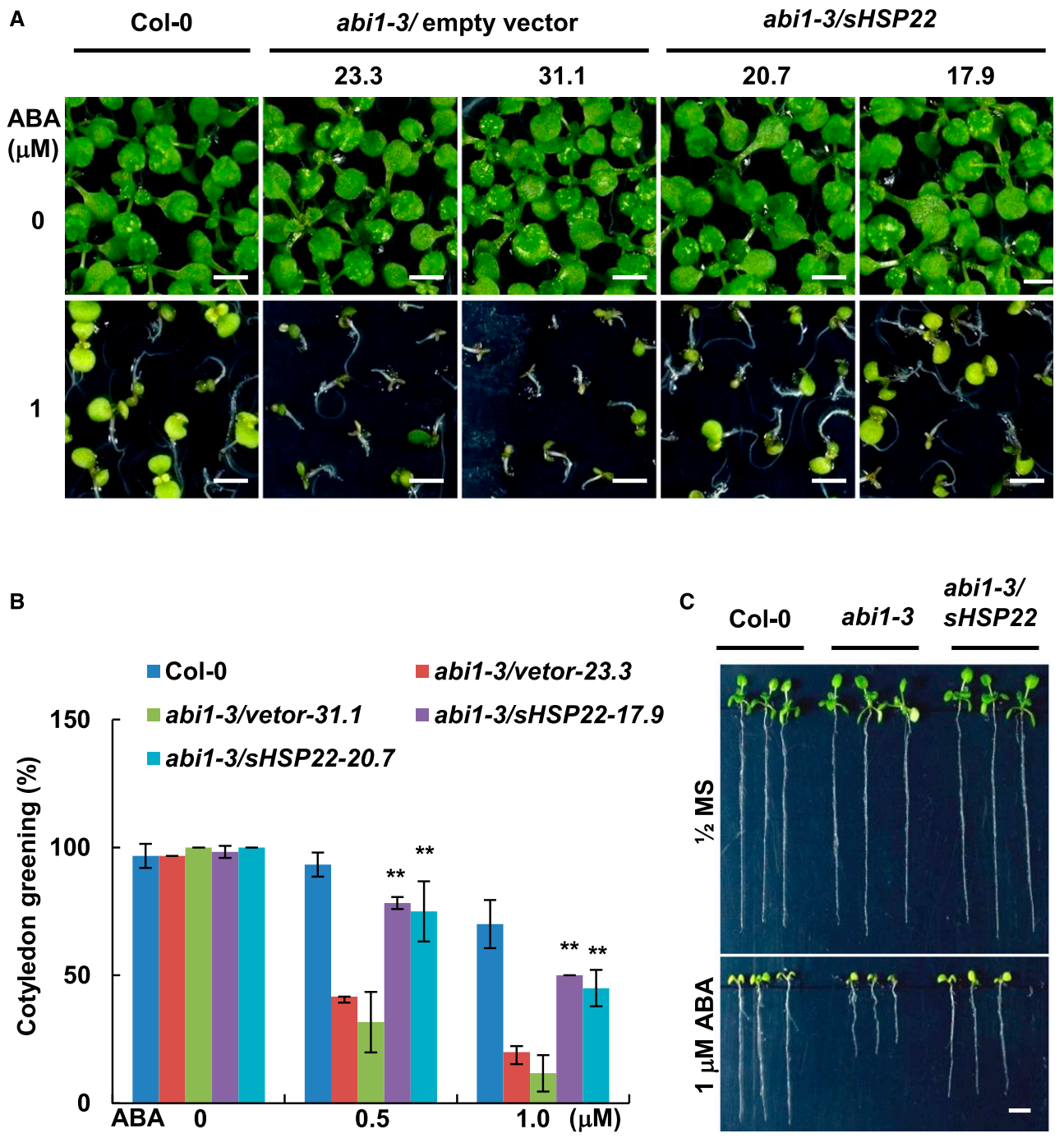

Figure 6. *sHSP22* can partially rescue ABA hypersensitivity of *abi1-3*. A, Cotyledon greening phenotype of Col-0, *abi1-3*, and *abi1-3/sHSP22* homologous plants in half-strength MS medium and medium supplemented with 1 μM ABA. Representative seedlings were shown 9 d after imbibition. Bar = 0.5 cm. B, Statistic analysis of cotyledon greening in half-strength MS medium containing various concentrations (0, 0.5, and 1.0 μM) of ABA. Col-0, *abi1-3*, and *abi1-3/sHSP22* complementation plants were germinated and grown for 9 d. The values are the means ± SD of triplicate repeats ($n = 90$, $^{**}P < 0.01$). C, Root phenotype of representative seedlings grown on half-strength MS medium without or with 1 μM ABA shown in A. Bar = 0.5 cm.

1 μM NPA, an auxin efflux facilitator inhibitor, high temperature-triggered hypocotyl elongation of *sHSP22 OX* was suppressed (Fig. 7D), suggesting that *sHSP22* might be involved in auxin transport. To explore whether *ABI1* is required for temperature-induced hypocotyl elongation of *sHSP22 OX*, we analyzed hypocotyl elongation of vector control, *sHSP22 OX*, *abi1-3*, and *abi1-3/sHSP22 OX* plants. With similar short

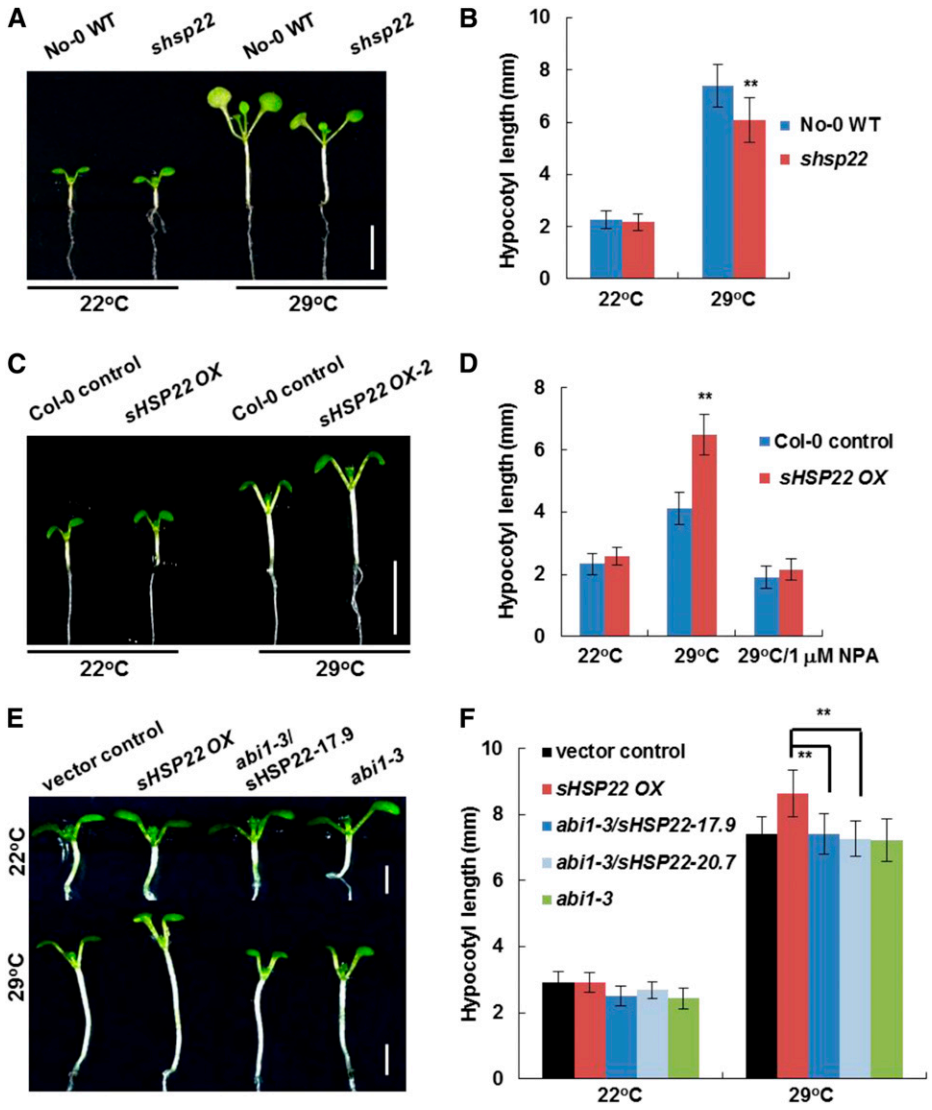

Figure 7. *sHSP22* can promote hypocotyl elongation at high temperature. A, Hypocotyl elongation of 6-d-old No-0 wild type and *shsp22* mutant grown at 22°C and 29°C. Plants were grown at 22°C for 2 d before being transferred to 29°C for 4 d. Bar = 0.5 cm. B, Quantitative analysis of hypocotyl length in seedlings shown in A. Values are means ± SD (n = 40), $^{**}P < 0.01$. C, Hypocotyl elongation of 6-d-old *sHSP22* transgenic and vector control plants grown at 22°C and 29°C. Plants were grown at 22°C for 2 d before being transferred to 29°C for 4 d. Bar = 0.5 cm. D, Quantitative analysis of hypocotyl length of 6-d-old *sHSP22* transgenic and vector control plants grown in half-strength MS medium supplemented with 0 and 1.0 μM NPA at 22°C and 29°C, respectively. The values are means ± SD (n = 40), $^{**}P < 0.01$. E, Hypocotyl elongation of 6-d-old *sHSP22 OX*, vector control, *abi1-3*, and *abi1-3/sHSP22* plants grown at 22°C and 29°C. Plants were grown at 22°C for 2 d before being transferred to 29°C for 4 d. Bar = 0.2 cm. F, Quantitative analysis of hypocotyl length in seedlings shown in E. Values are means ± SD (n = 40), $^{**}P < 0.01$.

hypocotyls at 22°C, *abi1-3* and *abi1-3/sHSP22 OX* developed an average of 7.2 mm hypocotyl at 29°C comparable to vector control (Fig. 7, E and F).

To dissect the molecular mechanism of *sHSP22* action in the auxin-mediated hypocotyl elongation response, we first measured the free IAA levels in hypocotyls of 6-d-old vector control and *sHSP22 OX* seedlings grown at 22°C and 29°C. Whereas there was no significant difference between *sHSP22 OX* and vector control at 22°C, an obvious increase of the free IAA concentration was observed in the hypocotyls of *sHSP22 OX* when seedlings were grown at 29°C (Fig. 8A). Secondly, we investigated the expression levels of auxin signaling marker genes *SHY2/IAA3* as well as *IAA19*, which act in hypocotyl development, in vector control and *sHSP22 OX* lines (Tatematsu et al., 2004; Sun et al., 2012). Higher expression of both genes was observed in hypocotyls of *sHSP22 OX* at 29°C compared with that of vector control plants (Fig. 8B).

Taken together, these data suggest that *sHSP22* modulates the auxin response through a change in auxin concentration and affecting auxin response.

sHSP22 Affects Accumulation of Auxin Efflux Facilitator PIN Proteins

Auxin polar transport tuned by differential membrane-localized influx and efflux carriers modulated Arabidopsis development (Vanneste and Friml, 2009). Thus, we tested whether *sHSP22 OX* lines affect auxin polar transport in roots by applying phytotropin NPA, an auxin efflux facilitator inhibitor (Ruzicka et al., 2010). *sHSP22 OX* seedlings transferred to medium containing 1 μM NPA had 57.2% reduced primary root length, while control plants had 25.57% reduced primary root length (Fig. 9, A and B). NPA functions through undefined membrane-localized NPA-binding

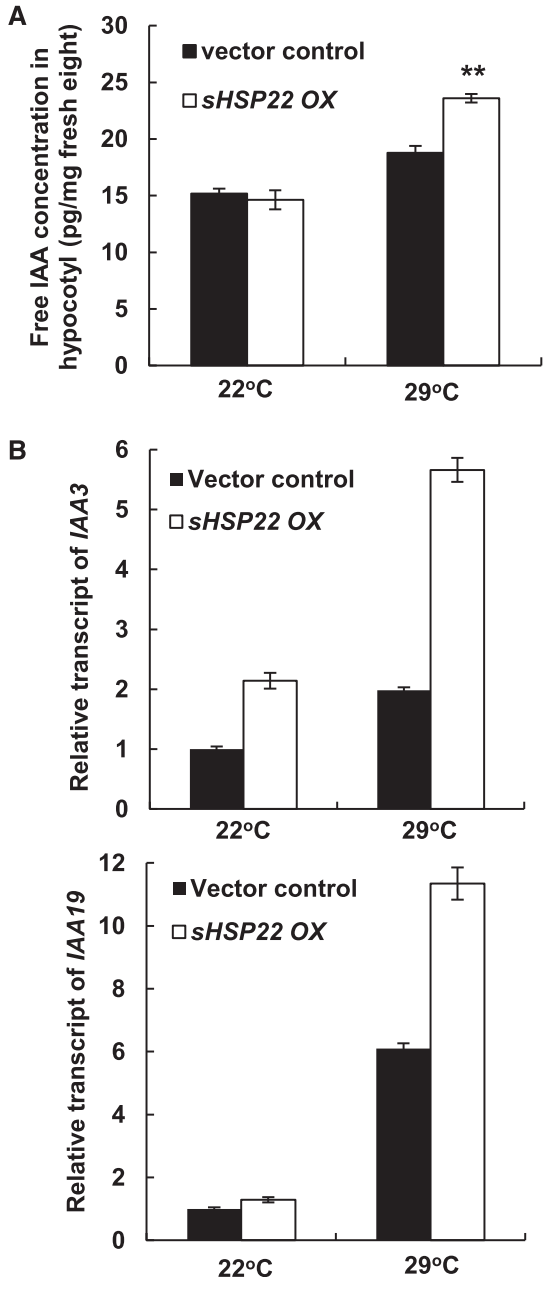

Figure 8. Measurement of IAA content and auxin-inducible *Aux/IAA* gene expression in *sHSP22 OX* and vector control. A, IAA concentration in hypocotyls of 6-d-old *sHSP22* transgenic and vector control plants grown at 22°C and 29°C. Plants were grown at 22°C for 2 d before transferred to 29°C for 4 d. Values are means ± SD of three replicate repeats. $^{**}P < 0.01$. B, Relative transcript abundance of auxin-responsive *IAA3* and *IAA19* by qRT-PCR in hypocotyls of *sHSP22* transgenic and vector control plants. Transcript levels of *IAAs* were normalized to the *ACTIN2* expression and were relative to that of untreated vector control seedlings. Error bars represent ± SD of three replicate repeats.

proteins to inhibit auxin efflux carriers activity (Cox and Muday, 1994; Bailly et al., 2008). Thus, we introduced primary auxin efflux transporter PIN reporters, including *proPIN1:PIN1-GFP*, *proPIN2:PIN2-GFP*, *proPIN3:PIN3-GFP*, *proPIN4:PIN4-GFP*, *proPIN7:PIN7-GFP*, and auxin response reporter *DR5rev:GFP* into *sHSP22 OX* through genetic crossing to detect whether these auxin efflux facilitators were affected by *sHSP22*. Previous findings showed that shoot-derived auxin flows toward the root tip, facilitated by basally localized PIN1, PIN3, PIN4, and PIN7 in the stele, and reaches a maximum at the quiescent center (QC) and columella initials and then is redirected upward by apically localized PIN2 in the epidermis (Petrásek and Friml, 2009). While no altered polar localization of PIN1, PIN3, PIN4, and PIN7 in *sHSP22 OX* was observed, the GFP fluorescence of PIN1, PIN3, PIN4, and PIN7 all exhibited considerable decrease in the root tips of 5-d-old *sHSP22 OX* homozygous lines compared with Col-0, which indicated reduced accumulation of basally localized PIN1, PIN3, PIN4, and PIN7 in root tip of *sHSP22 OX* (Fig. 9, D and G). On the other hand, unaltered apically localized but slightly accumulated PIN2 was observed in the *sHSP22 OX* root apex (Fig. 9, E and G). Additionally, the *DR5rev:GFP* fluorescence intensity decreased in QC and columella cells of *sHSP22 OX* compared with Col-0 (Fig. 9, F and G). This phenomenon presumably resulted from less acropetal and slightly greater basipetal auxin transport mediated by a variety of polarly localized PINs.

To rule out the possibility that the changes in PIN accumulation were due to transcriptional regulation, we examined expression of the corresponding *PINs* seedlings (Fig. 9D). In contrast to the reduced accumulation of PIN1, PIN3, PIN4, and PIN7 in *sHSP22 OX*, comparable *PIN3* expression and increased *PIN1*, *PIN4*, and *PIN7* transcription were observed (Supplemental Fig. S10), which suggests that *sHSP22 OX* decreased the accumulation of basally localized PINs is independent of transcriptional regulation. Moreover, the distribution of GFP fused sHSP22 driven by the *35S* promoter revealed punctate fluorescence in the stele, which spread into the columella as well as the lateral root cap (Fig. 9C), and overlapped with the PIN proteins distribution. On the contrary, PIN1, PIN3, and PIN7 displayed increased fluorescence intensity in *shsp22* while PIN2 displayed decreased fluorescence intensity (Fig. 10, A and B).

Taken together, these data indicate that sHSP22 plays an important role in specifically modulating auxin transport efflux carriers.

sHSP22 OX Potentiates PIN1 Trafficking and Initiates More Lateral Roots

Auxin efflux PIN proteins have been shown to undergo constitutive subcellular cycling of endocytosis and recycling back to the plasma membrane (Kleine-Vehn and Friml, 2008; Friml, 2010). The fungal toxin brefeldin A (BFA) specifically inhibits a subclass of exchange factors for ARF-GTPases, and as a consequence blocks PIN protein trafficking from the endosome to plasma membrane

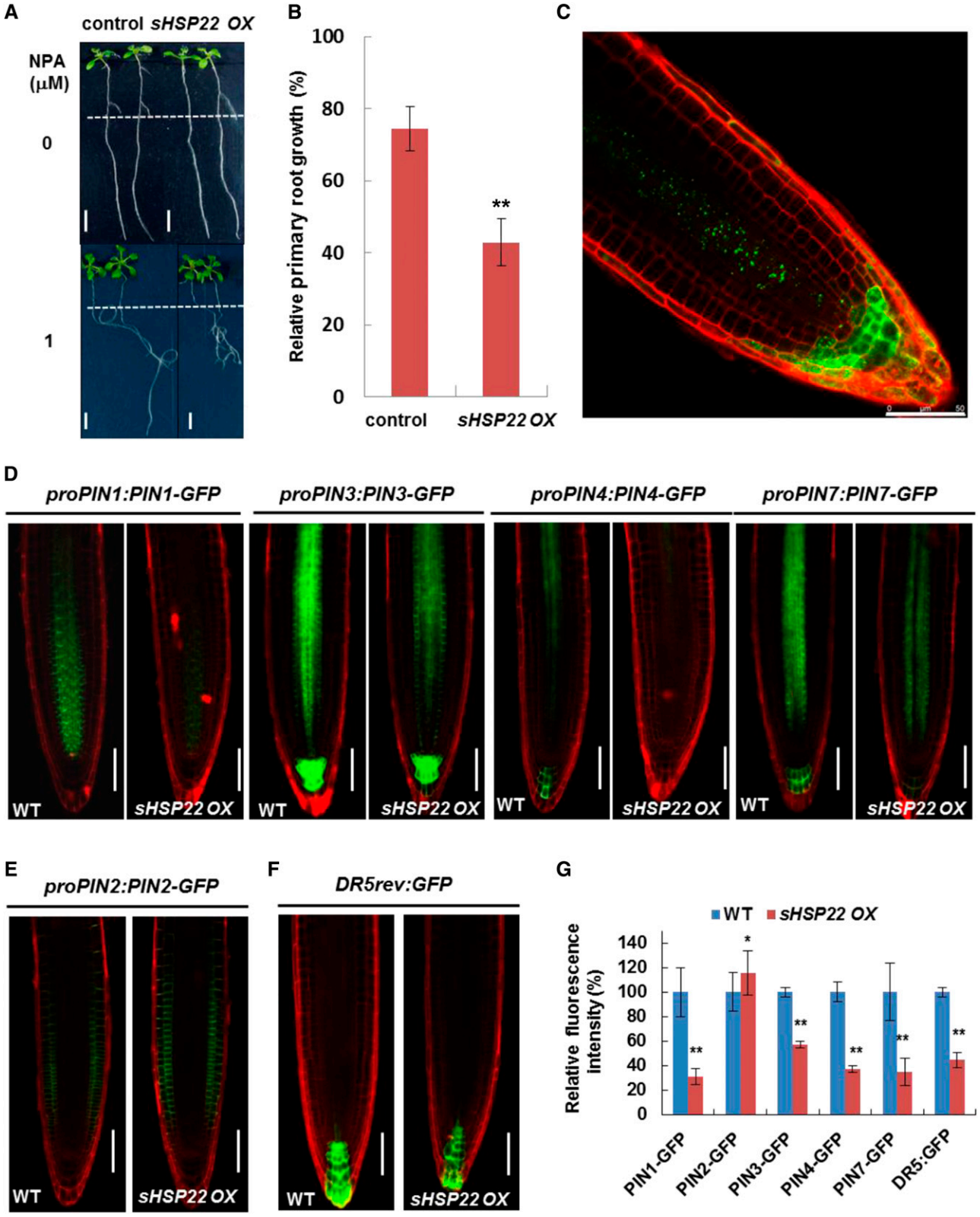

Figure 9. *sHSP22 OX* shows enhanced sensitivity to NPA and affects accumulation of PIN proteins. A, *sHSP22* overexpression and vector control seedlings germinated vertically for 5 d with similar roots length were transferred to half-strength MS medium with or without 1 μM NPA and grown in a vertical position for additional 7 d (top) or 11 d (bottom). The dashed lines denote root length when transferred. Bar = 0.5 cm. B, Statistical analysis of the primary root growth in seedlings shown in A. The relative root

and results in endosomal BFA compartment formation (Geldner et al., 2001, 2003). Thus, we examined whether sHSP22 interferes with trafficking of representative PIN1 to reduce its basal plasma membrane localization. Before BFA treatment, reduced basally localized PIN1 was shown in *sHSP22 OX* compared with Col-0. When treated with 50 μM BFA, basally localized PIN1 progressively disappeared from the plasma membrane and BFA bodies were observed in Col-0 1 h later. In contrast, BFA-induced PIN1 internalization was more rapid in *sHSP22 OX*, and more BFA bodies were observed after the same treatment time (Fig. 11A), which shows BFA-sensitive PIN1 trafficking in the *sHSP22 OX* roots.

Based on accumulation of decreased basally localized PIN1, PIN3, PIN4, and PIN7 and slightly increased apically localized PIN2 in *sHSP22 OX* in Figure 9, D and E, we reasoned that these changes may affect lateral root development. Therefore, we measured lateral root formation in *sHSP22 OX* in the presence of exogenous auxin. *sHSP22 OX* developed significantly more lateral roots after either 50 nM NAA or in response to an increasing concentration of IAA (Fig. 11, B and C). Moreover, we checked the expression levels of *GATA23* and *SKP2B* that play vital roles in founder cell specification (De Rybel et al., 2010; Manzano et al., 2012) in roots of the vector control and *sHSP22 OX*. The transcript abundance of *GATA23* and *SKP2B* in *sHSP22 OX* was comparable to that in vector control without IAA treatment; however, the expression level of *GATA23* was induced markedly by IAA treatment at 2 h and the moderate induction of *SKP2B* occurred at 4 h by IAA treatment in *sHSP22 OX* (Fig. 11D). This suggested *sHSP22 OX* could trigger more lateral root emergence upon IAA treatment.

DISCUSSION

Auxin Integrates ABI1 to Regulate Lateral Root Formation

Lateral root (LR) development enables plants to react with flexibility and adaptability to changes in environmental conditions. Researchers have shown that auxin is the key instructive signal for LR development, and ABA signaling exerts an antagonistic function (Fukaki and Tasaka, 2009). However, the means by which ABA signaling cascades interact with auxin biosynthesis, metabolism, signaling, or distribution remain unclear. By screening ABA signaling mutants in response to exogenous auxin, we report that both the *ABI1* loss-of-function and knockdown mutants exhibited less sensitivity in LR formation upon with exogenous auxin application (Fig. 1; Supplemental Fig. S1). These observations suggested that ABI1 is an interaction node for auxin to integrate with ABA and regulate LR formation. Consistent with this notion, an auxin-inducible chimeric reporter *proDc3:GUS* from *Daucus carota* showed significantly less GUS expression in the roots of Arabidopsis-dominant negative *abi1-1*mutant (Rock and Sun, 2005), which supports that the auxin-responsive expression is dependent on *ABI1*. Moreover, genome-wide gene expression profiling in Arabidopsis wild type and *abi1-1* showed the down-regulation of *GH3.5* and *HAM4*, which encode an IAA-amino conjugation synthase and a SCARECROW transcription factor, respectively (Hoth et al., 2002). It is reasonable to speculate that decreased expression of these two genes in *abi1-1* modulated auxin homeostasis (Staswick et al., 2005) as well as changes in the specification of QC and stem cell niches (Engstrom et al., 2011).

Previous research showed that the ABA signaling component ABI3, which is farnesylated by ERA1, is essential for auxin-mediated LR formation (Brady et al., 2003), presumably due to uncharacterized auxin responsive targets bound by ABI3 (Nag et al., 2005). As *ABI1* genetically acts upstream to regulate *ABI3* (Parcy and Giraudat, 1997), impaired auxin-induced LR formation in *abi1-3* could be a consequence of altered transcription abundance of *ABI3*. On the other hand, another ABA signaling component ABI4 inhibits LR formation through modulation of auxin polar transport (Shkolnik-Inbar and Bar-Zvi, 2010), distinct from auxin signaling regulation of ABI3. Whether ABI1 affects auxin polar transport related to ABI4 remains unclear. Nevertheless, these findings provide evidence that ABA signaling influences auxin signaling and distribution.

Given the versatile targets and multiple regulators of *ABI1* in ABA signaling, we identified a sHSP encoding gene, *sHSP22*, which requires ABI1 for IAA induction (Fig. 2, A–C). A subsequent physiological investigation showed that *shsp22* and *sHSP22 OX* lines exhibited auxin-associated phenotypes, including involvement in high temperature-mediated hypocotyl elongation (Fig. 7, A–D), increased sensitivity of *sHSP22 OX* plants to exogenous auxin and auxin transport inhibitor application (Figs. 9A and 11, A and B). Furthermore, *sHSP22* is involved in auxin-related hypocotyl elongation at high

Figure 9. (*Continued.*)
growth percentage in NPA was normalized to that in half-strength MS medium. Error bars represent ±SD ($n = 30$), $^{**}P < 0.01$. C, The distribution and localization of sHSP22-GFP recombinant protein in root tips of 5-d-old T3 homozygous transgenic Arabidopsis seedlings. D, Distribution of *proPIN1:PIN1-GFP, proPIN3:PIN3-GFP, proPIN4:PIN4-GFP, proPIN7:PIN7-GFP* in Col-0, and *sHSP22* overexpressing plants 4 d after germination. PI was used to stain the cell wall. Bar = 75 μm. E, Distribution of *proPIN2:PIN2-GFP* in Col-0 and *sHSP22*-overexpressing plants 4 d after germination. PI was used to stain the cell wall. Bar = 75 μm. F, Expression pattern of synthetic *DR5rev:GFP* reporter in Col-0 and *sHSP22* overexpressing plants 4 d after germination. PI was used to stain the cell wall. Bar = 75 μm. G, Statistical analysis of fluorescence intensity for roots shown in D to F. Relative fluorescence intensity percentage in *sHSP22* overexpressing plants was normalized to that in wild type as 100%. Error bars represent ±SD ($n = 10$), $^{*}P < 0.05$ and $^{**}P < 0.01$.

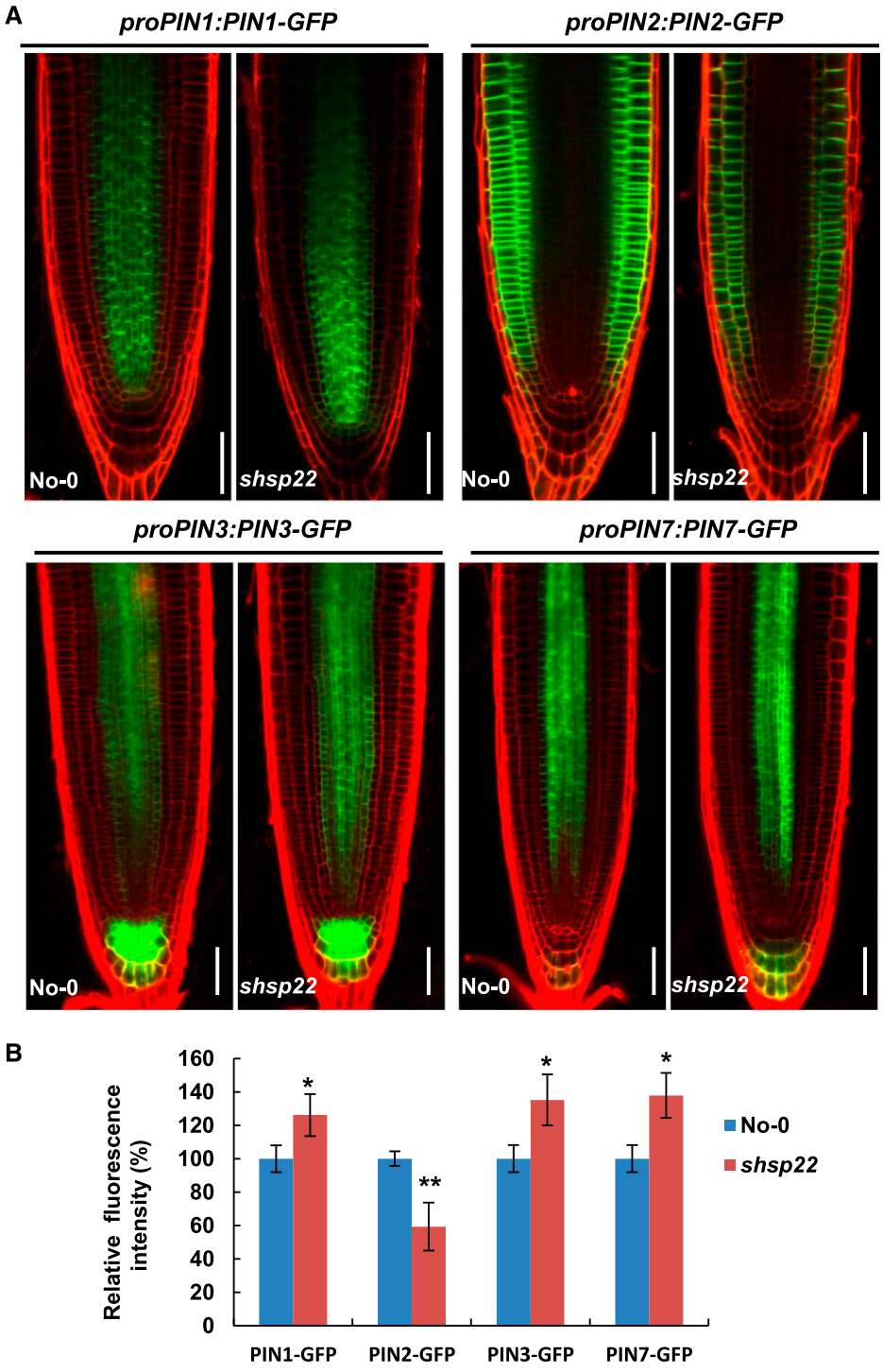

Figure 10. The distribution of PIN proteins in *shsp22*. A, Distribution of *proPIN1:PIN1-GFP*, *proPIN2:PIN2-GFP*, *proPIN3:PIN3-GFP*, and *proPIN7:PIN7-GFP* in the roots of No-0 and *shsp22* 4 d after germination. PI was used to stain the cell wall. Bar = 50 μm. B, Statistics analysis of fluorescence intensity for roots shown in A. Relative fluorescence intensity percentage in *shsp22* plants was normalized to that in No-0 as 100%. Error bars represent $\pm$SD (n = 10), *$P < 0.05$ and **$P < 0.01$.

temperature (Fig. 7). Collectively, this suggests that *sHSP22* functions in the auxin response and provides a clue for deciphering ABA and auxin crosstalk.

sHSP22 Exerts Negative Effects on ABA Signaling

The family of sHSPs in Arabidopsis comprises 19 members, which far exceeds other organisms (Haslbeck et al., 2005), suggesting that sHSPs diverged in certain cell types and organelles for specific roles that still need to be unraveled. Because expression of single ER-localized *sHSP22* was induced by ABA treatment (Fig. 2D), we speculated a specific function for *sHSP22* in ABA response. Using a reverse genetics approach, further phenotypic analyses showed that *sHSP22* exerts negative effects on ABA-inhibited cotyledon greening and root growth (Figs. 3 and 4). Intriguingly, overexpression plants of a truncated sHSP22-D lacking

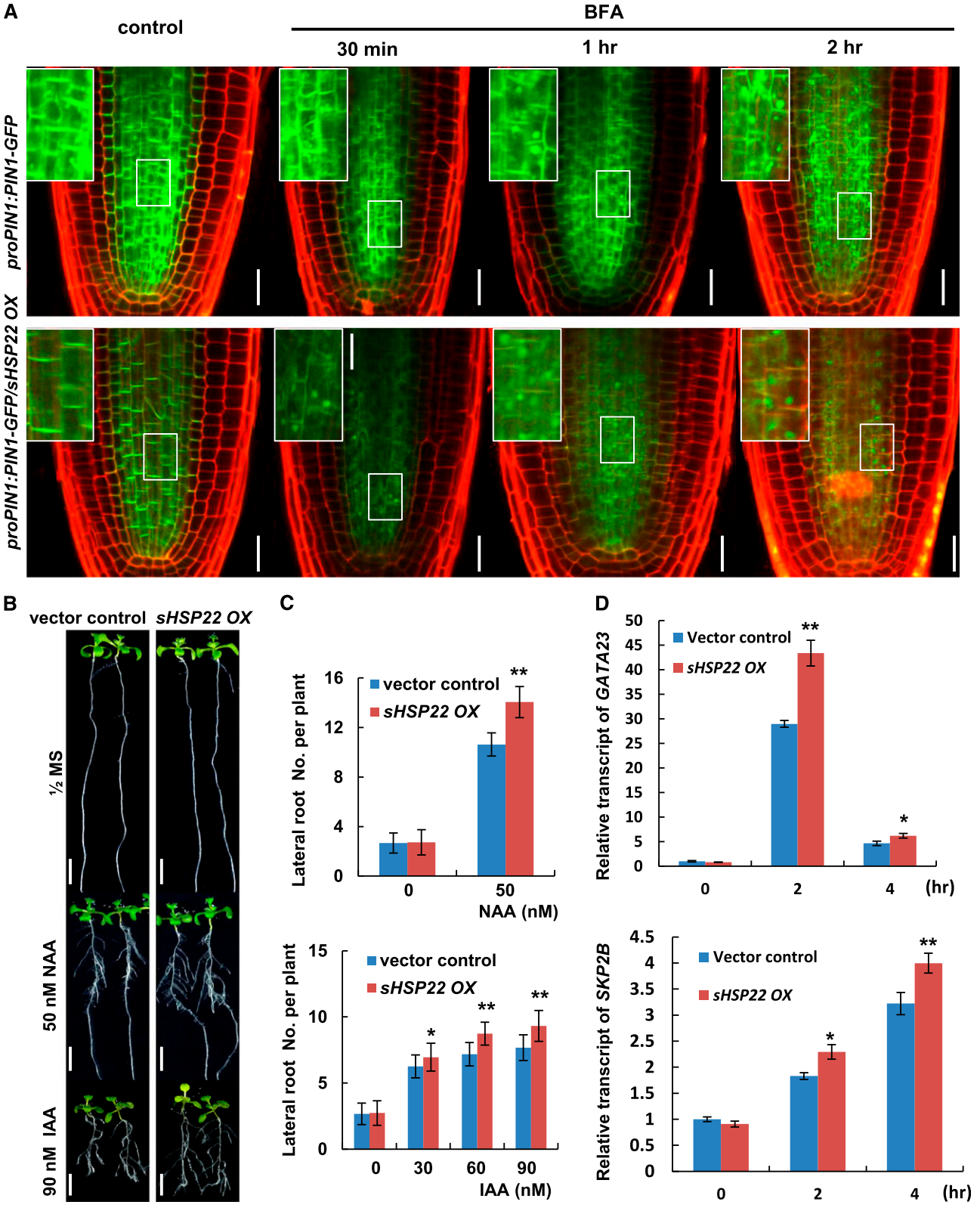

Figure 11. *sHSP22 OX* potentiates PIN1 trafficking and initiates more lateral roots. A, Internalization of *proPIN1:PIN1-GFP* in 5-d-old Col-0 and *sHSP22* overexpressing Arabidopsis seedling roots upon adding a vesicle-trafficking inhibitor using 50 μM BFA for the indicated times. Inserted panels are a magnification of the denoted area. PI was used to stain the cell wall. Bar = 20 μm. B, *sHSP22* overexpression and vector control seedlings germinated vertically for 5 d with similar length of roots were transferred to

signal peptide and ER retention sequence showed the similar response to wild type when treated with ABA (Fig. 5; Supplemental Fig. S8). Taken together, the active sHSP22 localized in the ER accounts for the reduced sensitivity of *sHSP22 OX* to ABA. We hypothesized that sHSP22 is involved in ER quality control to respond to ABA. Various stressful conditions trigger ABA production and signaling, accompanied by the accumulation of denatured structural and functional proteins in ER. sHSP22 may act as a molecular chaperone as an oligomer to bind and prevent unfolded protein from aggregating, which protects plants from cellular protein malfunction and stress. In accordance with this hypothesis, a putative ER sHSP alleviates ER stress in transgenic tomato (*Solanum lycopersicum*; Zhao et al., 2007). Moreover, ER stress induces phosphorylation of its human ortholog HSP27, which results in HSP27 binding to polyubiquitinated proteins for proteasome degradation (Parcellier et al., 2003). No such role for sHSP22 has been observed in Arabidopsis; however, the identification of sHSP22 as a ubiquitination target through proteomic analyses supports this possibility (Kim et al., 2013).

To dissect the relationship between *sHSP22* and ABA signaling components, we found that *sHSP22* partially rescues *abi1-3* ABA hypersensitivity in cotyledon greening and root growth (Fig. 6).

sHSP22 Modulates Polar Auxin Transport and Shows Versatile Auxin Phenotype

We elucidated a scenario of sHSP22 action in comprehensive aspects of auxin-associated plant development. Initially, *sHSP22* integrates high temperature cue to mediate auxin-triggered hypocotyl elongation (Fig. 7). Recent research has discerned light-perceived PIF4 regulation of auxin biosynthesis in this process (Franklin et al., 2011; Sun et al., 2012), and our results highlight the high temperature-induced role of sHSP22 related to auxin polar transport. This notion is implicit in the abolished phenotype of *sHSP22 OX* upon NPA application (Fig. 7D), along with obvious changes in free auxin levels and expression of the auxin signaling marker genes *IAA3* and *IAA19* in *sHSP22 OX* and vector control plants (Fig. 8). Further direct evidence was generated from dissecting *sHSP22 OX* increased root growth sensitivity to NPA, reduced accumulation of basal plasma membrane-localized PINs essential for auxin acropetal transport in the root apex (Fig. 9), and potentiated PIN1 trafficking in response to vesicle trafficking inhibitor BFA (Fig. 11A). Taken together, these physiological and genetic data support a role for sHSP22 in regulating auxin polar transport.

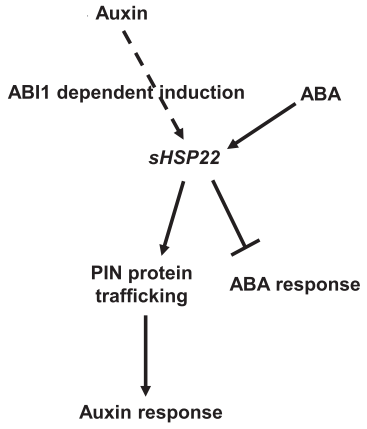

Figure 12. Hypothesized model of sHSP22 action in auxin and ABA crosstalk. Auxin induced the expression of *sHSP22* is dependent on *ABI1*. sHSP22 affects PIN protein trafficking to modulate auxin response while negatively regulates ABA response. Positive interactions are denoted by an arrow; bars indicate repression effects.

However, how the ER-localized sHSP22 elaborately modulates accumulation and trafficking of plasma membrane PINs remains a mystery. Current progress in identifying ER-localized PIN transporters and elucidating of PIN vesicle trafficking routes provides clues for addressing this question. On one hand, the ER-localized PINs, PIN5, PIN6, PIN8, and PIN-LIKES PILS2, PILS5, prominently function in intracellular auxin homeostasis and metabolism and presumably increase auxin accumulation in the ER to regulate plant development (Mravec et al., 2009; Barbez et al., 2012; Ding et al., 2012; Cazzonelli et al., 2013). Whether sHSP22 interacts with these ER-localized PINs to lead to coordination of plasma membrane-localized PINs remains unclear. On the other hand, crucial auxin transporter PINs undergo constitutive trafficking through secretion, endocytosis, transcytosis, and sorting for polar plasma membrane localization (Friml, 2010). Whether sHSP22 affects PIN vesicle trafficking at the sorting or vacuolar degradation steps and the necessary vesicle trafficking machinery components, and how this process orchestrates environmental cues, such as high temperature and abiotic stress, are further issues that should be explored.

Overall, based on our data, we present a working model of sHSP22 action in ABA and auxin signaling crosstalk (Fig. 12). ABI1 is a negative regulator of ABA signaling (Gosti et al., 1999), sHSP22 acts to exert

Figure 11. (*Continued.*)
half-strength MS medium containing 0 and 50 nM NAA and 90 nM IAA and grown in a vertical position for additional 7 d. Bar = 0.5 cm. C, Statistic analysis of lateral root number of seedling shown in B. Error bars represent ± SD ($n = 30$), $^{**}P < 0.01$ and $^{*}P < 0.05$. D, Expression of *GATA23* and *SKP2B* in vector control and *sHSP22 OX* seedlings. One-week-old vector control and *sHSP22 OX* seedlings were treated with 2 μM IAA for 0, 2, and 4 h, and the excised roots were harvested for RNA extraction and qRT-PCR. Transcript levels were normalized to *ACTIN2* expression, and error bars represent ±SD of triplicates. $^{**}P < 0.01$ and $^{*}P < 0.05$.

negative effects on ABA signaling, exhibiting versatile responses in seed germination and seedling establishment. Furthermore, ABI1 is also required for auxin-mediated lateral root formation and auxin-induced *sHSP22* expression, and *sHSP22* is involved in auxin-related hypocotyl elongation at high temperature. Additionally, sHSP22 potentiates auxin efflux facilitator PIN proteins trafficking to enhance auxin signaling, which leads to increased sensitivity in root growth to NPA and lateral root development to exogenous auxin. ABI1-sHSP22 provides a module for orchestrating ABA and auxin signaling, which is important for plant development and environment adaptation.

MATERIALS AND METHODS

Plant Materials and Growth Conditions

The Arabidopsis (*Arabidopsis thaliana*) ecotypes Col-0 and No-0 were used for this study. The T-DNA insertion mutant SALK_076309, which was initially identified as *abi1-3* (Saez et al., 2006), was obtained from the Arabidopsis Biological Resource Center. The transposon-tagged mutant *shsp22* (psh16823) was obtained from the RIKEN Bioresource Center. Certain plant materials used in this study were previously described: *DR5rev:GFP* (Friml et al., 2003), *proPIN1:PIN1:GFP* (Benková et al., 2003), *proPIN2:PIN2:GFP* (Blilou et al., 2005), *proPIN3:PIN3:GFP* (Blilou et al., 2005), *proPIN4:PIN4:GFP* (Vieten et al., 2005), and *proPIN7:PIN7:GFP* (Blilou et al., 2005).

The seeds were surface sterilized with 10% bleach and washed three times with sterile water. The sterile seeds were suspended in 0.2% agarose and plated on half-strength Murashige and Skoog (MS; Duchefa Biochemie) medium. The seeds were stratified in the darkness for 3 d at 4°C and then transferred to a tissue culture room at 22°C under a 16-h-light/8-h-dark photoperiod (light intensity 60 μmol m^{-2} s^{-1}). The half-strength MS medium was supplemented with 1.5% Suc and with ABA as needed. For root growth measurements, half-strength MS medium containing 2% Suc was used to promote lateral root development (Zhang et al., 1999).

Transformation Vectors and Construction of Transgenic Plants

To obtain the *35S-myc-sHSP22* overexpression vector, a 588-bp *Kpn*I-*sHSP22-Bam*HI fragment containing the full-length *sHSP22* CDS (Arabidopsis Genome Initiative locus At4g10250) was cloned into pCAMBIA-1300-221-myc (Liu et al., 2010) under control of the *35S* promoter. Analogously, the *35S-myc-sHSP22-D* overexpression vector was constructed by amplifying a 516-bp *Kpn*I-*sHSP22-D-Bam*HI fragment containing *sHSP22* CDS with the N-terminal signal peptide and C-terminal ER retention peptides deleted, then cloning into pCAMBIA-1300-221-myc. (*Myc-sHSP22-D*-Fw:5′-GGGGTACCCATGAGTGAAGGGTCTTTGTC-3′; *Myc-sHSP22-D*-Rev:5′-CGGGATCCTCATTCAGAAGAGCTGATTT-3′). For *sHSP22*-fused GUS driven by the *sHSP22* promoter, a 949-bp promoter region just upstream of the *sHSP22* ATG start codon followed by the *sHSP22* CDS was amplified and cloned into *Pst*I-*Bam*HI sites in the binary vector pCAMBIA-1300-221. For the *shsp22* complementation vector, the *sHSP22* genomic sequence driven by the *sHSP22* promoter was amplified and cloned into pCAMBIA2300 *Pst*I-*Sac*I sites. For *sHSP22-GFP*, the *sHSP22* coding sequence fused to the N terminus of *GFP* under control of the 35S promoter was cloned into *Kpn*I-*Bam*HI sites in pCAMBIA-1300-221-GFP (Liu et al., 2010). For *sHSP22-D-GFP*, the *sHSP22-D* coding sequence fused to the N terminus of *GFP* under control of the 35S promoter was cloned into *Xba*I-*Kpn*I sites in pCAMBIA-1300-221-GFP (Liu et al., 2010).

Arabidopsis was transformed using the floral dip method (Zhang et al., 2006) using *Agrobacterium tumefaciens* strains EHA105 and GV3101. For the phenotypic analysis, T3 or T4 homozygous lines were used.

Primary Root Length Measurement and Lateral Root Number Count

For the root growth assay, seeds were germinated and grown on vertical plates for 5 d, then plants with similar root lengths were transferred to half-strength MS medium containing different concentrations of auxin, ABA, or polar auxin transport inhibitor NPA and grown for additional days to observe the root phenotypes. Plants were photographed using a camera Canon 550D, the primary root lengths were measured using the software Image J, and the lateral root (emergence from primary root) number was counted under an inverted microscope (MOTIC, SMZ-168). The hypocotyl elongation measurements for wild-type, *shsp22*, and *sHSP22 OX* seedlings at 22°C and 29°C were the same as measurements of the primary root length.

Phylogenetic Analysis

The sHSP22 amino acid sequence was used to query homologs from the National Center for Biotechnology Information database (http://www.ncbi.nlm.nih.gov/) and the Arabidopsis Information Resource (http://www.arabidopsis.org/index.jsp) using BLAST. The amino acid sequences were aligned using ClustalX2 with default settings. Next, the phylogenetic tree was constructed using the neighbor-joining method with a bootstrap test for phylogeny set with 5,000 replicates in MEGA version 4.0.

Verification of Transposon-Tagged *shsp22* Mutant

The transposon-tagged mutant *shsp22* (psh16823) seeds were ordered from Riken Bioresource Center (Japan). Homozygous mutant was identified using PCR from genomic DNA using forward primer (P1, 5′-CATGATGAAGCACTTGC-3′), transposon specific primer (Ds3-2a, 5′-CCGGATCGTATCGGTTTTCG-3′), and reverse primer (P2, 5′-CACCTTCCCCTGTTAAGGAAG-3′). To identify whether *shsp22* is a knockout mutant, RNA was extracted from 2-week-old No-0 and *shsp22* seedlings, digested by DNase I, and subjected to reverse transcription followed by PCR using specific primers to amplify *sHSP22* CDS, with *ACTIN1* as an internal control. *RT* Fw: ATGATGAAGCACTTGCTAAGCA; *RT* Rev: TCAGAGTTCTTTGGATTCAGAAG; *ACTIN1* Fw: CATCAGGAAGGACTTGTACGG; *ACTIN1* Rev: GATGGACCTGACTCGTCATAC.

RNA Gel Blotting

Total RNA was isolated from 2-week-old Col-0, an empty vector, and *sHSP22 OX* homozygous transgenic plants and separated by agarose gel electrophoresis, and then the samples were then transferred to Hybond N^+ nylon membranes (Amersham Pharmacia Biotech) through upward capillary transfer in a 10× SSC solution. The membranes were stained with methylene blue and hybridized at 65°C as described (Chen et al., 2010) with a PCR fragment that corresponds to 111 to 550 bp of *sHSP22* as a probe labeled with [α-^{32}P]dCTP.

Immunoblotting

Immunoblotting for Myc-sHSP22 and truncated Myc-sHSP22-D expression in transgenic Arabidopsis was performed as described previously (Liu et al., 2010), with a primary anti-c-myc antibody (9E10; Santa Cruz Biotechnology,1:1,000) followed by secondary goat anti-mouse antibody conjugated to horseradish peroxidase and visualized using chemiluminescence as instructed by the manufacturer (Amersham Pharmacia).

Subcellular Localization

For the subcellular localization analyses, *A. tumefaciens*–mediated transient expression of sHSP22 fused to GFP driven by the 35S promoter was generated using a previously described agroinfiltration method in *Nicotiana benthamiana* (Liu et al., 2010). To investigate whether sHSP22 and sHSP22-D were localized in ER, equal volume suspensions of *Agrobacterium* strain EHA105 harboring Ti plasmids expressing both sHSP22-GFP and RFP-HDEL or sHSP22-D-GFP and RFP-HDEL (Napier et al., 1992) were mixed (final OD_{600} = 0.75), coinfiltrated into *N. benthamiana* leaves, and visualized using a Leica TCS SP5 confocal laser scanning microscope 3 d later.

GUS Bioassays

Histochemical staining for GUS activity was performed using a method previously described (Zhang et al., 2007). Whole seedlings or different tissues with or without hormone treatment were immersed in the GUS staining solution (1 μg/mL X-glucuronidein, 100 mM sodium phosphate, pH 7.0, 0.5 mM ferricyanide, and 0.03%Triton X-100), incubated at 37°C in the dark for 20 min

to several hours depending on the experimental requirement, and then distained in 70% ethanol. The materials were cleared using HCG solution (chloroacetaldehyde:water:glycerol = 8:3:1) for 30 s and observed using the Leica Microsystems DM5000B microscope.

Confocal Microscopy Observation

Roots of 5-d-old plants were mounted in a 10 μM propidium iodide solution for 3 to 5 min for laser confocal scanning microscopy (TCS SP5; Leica). The fluorescence excitation and emission wavelengths for GFP were 488 and 510 nm, and for propidium iodide (PI) were 543 and 620 nm. The fluorescence was quantified using the LAS AF Lite program on confocal sections acquired using the same microscope settings. Approximately 10 images were examined, and at least three independent experiments were performed. The statistical significance was evaluated by Student's test analysis.

Real-Time PCR Assays

Total RNA preparation, first-strand cDNA synthesis and real-time PCR were performed as previously described (Cui et al., 2012). DNase I-treated total RNA (2 μg) was denatured and subjected to reverse transcription using Moloney murine leukemia virus reverse transcriptase (200 units per reaction; Promega) at 42°C for 60 min. Real-time PCR was performed using SsoFast Eva Green Supermix (Bio-Rad) and the CFX96 real-time system (Bio-Rad). Gene expression was quantified at the logarithmic phase based on the expression of the housekeeping gene *ACTIN2* as an internal control. Three biological replicates were performed. Primer sequences for real-time PCR are shown in Supplemental Table S2.

Measurement of IAA Levels

Plants were grown at 22°C for 2 d before transfer to 29°C for 4 d in continuous light. Hypocotyls of 6-d-old *sHSP22* transgenic and vector control plants were harvested for the free IAA measurement. Approximately 200 mg (fresh weight) of tissues was collected for the IAA extraction and measurement using methods previously described (Zhou et al., 2010).

Accession Numbers

Arabidopsis Genome Initiative loci mentioned in this article are as follows: *HSP22* (At4g10250), *ABI1* (At4g26080), *HSP20* (At1g59860), *HSPB4* (NG_009823.1), *HSPB1* (NG_008995.1), *HSPB3* (NG_027758.1), *HSP26p* (NC_001134.8), *ABI3* (At3g24650), *ABI4* (At2g40220), *ABI5* (At2g36270), *PIN1* (At1g73590), *PIN2* (At5g57090), *PIN3* (At1g70940), *PIN4* (At2g01420), *PIN7* (At1g23080), *IAA3* (At1g04240), *IAA19* (At3g15540), *ACTIN1* (At2g37620), and *ACTIN2* (At3g18780).

Supplemental Data

The following supplemental materials are available.

Supplemental Figure S1. Lateral root development of *abi1-2* and *abi1-11* to exogenous auxin.

Supplemental Figure S2. Expression levels of *sHSP22* in *abi1-3* and associated mutants treated with or without 50 μM ABA.

Supplemental Figure S3. Expression pattern of *sHSP22* under different treatments.

Supplemental Figure S4. Relative expression of *sHSP22* in *shsp22* complementation plants.

Supplemental Figure S5. Generation and confirmation of *sHSP22* overexpression plants.

Supplemental Figure S6. *sHSP22* overexpression plants are less sensitive to ABA.

Supplemental Figure S7. Evolution relevance analysis for sHSP22 and its homologs in diverse species.

Supplemental Figure S8. ER localization of sHSP22 contributes to ABA response.

Supplemental Figure S9. Verification of *sHSP22* relative expression in *abi1-3/sHSP22* lines by qRT-PCR.

Supplemental Figure S10. Relevant gene transcription in wild-type and *sHSP22 OX* plants.

Supplemental Table S1. Differentially expressed genes in Col and *abi1-3*.

Supplemental Table S2. Primers used in this work.

ACKNOWLEDGMENTS

We thank Professor Judy Callis (University of California, Davis) for critically reading the manuscript and giving constructive suggestions. We also thank Drs. Jinfang Chu and Shuang Fang (National Centre for Plant Gene Research (Beijing) Institute of Genetics and Developmental Biology, Chinese Academy of Sciences) for determining the IAA content and Mr. Yanbao Tian (State Key Laboratory of Plant Genomics) for technical support.

Received August 28, 2017; accepted December 22, 2017; published December 29, 2017.

LITERATURE CITED

Bailly A, Sovero V, Vincenzetti V, Santelia D, Bartnik D, Koenig BW, Mancuso S, Martinoia E, Geisler M (2008) Modulation of P-glycoproteins by auxin transport inhibitors is mediated by interaction with immunophilins. J Biol Chem **283:** 21817–21826

Balogi Z, Cheregi O, Giese KC, Juhász K, Vierling E, Vass I, Vígh L, Horváth I (2008) A mutant small heat shock protein with increased thylakoid association provides an elevated resistance against UV-B damage in synechocystis 6803. J Biol Chem **283:** 22983–22991

Barbez E, Kubeš M, Rolčík J, Béziat C, Pěnčík A, Wang B, Rosquete MR, Zhu J, Dobrev PI, Lee Y, et al (2012) A novel putative auxin carrier family regulates intracellular auxin homeostasis in plants. Nature **485:** 119–122

Basha E, Friedrich KL, Vierling E (2006) The N-terminal arm of small heat shock proteins is important for both chaperone activity and substrate specificity. J Biol Chem **281:** 39943–39952

Belin C, Megies C, Hauserová E, Lopez-Molina L (2009) Abscisic acid represses growth of the Arabidopsis embryonic axis after germination by enhancing auxin signaling. Plant Cell **21:** 2253–2268

Benková E, Michniewicz M, Sauer M, Teichmann T, Seifertová D, Jürgens G, Friml J (2003) Local, efflux-dependent auxin gradients as a common module for plant organ formation. Cell **115:** 591–602

Bennett MJ, Marchant A, Green HG, May ST, Ward SP, Millner PA, Walker AR, Schulz B, Feldmann KA (1996) Arabidopsis *AUX1* gene: a permease-like regulator of root gravitropism. Science **273:** 948–950

Blilou I, Xu J, Wildwater M, Willemsen V, Paponov I, Friml J, Heidstra R, Aida M, Palme K, Scheres B (2005) The PIN auxin efflux facilitator network controls growth and patterning in Arabidopsis roots. Nature **433:** 39–44

Brady SM, Sarkar SF, Bonetta D, McCourt P (2003) The *ABSCISIC ACID INSENSITIVE 3* (*ABI3*) gene is modulated by farnesylation and is involved in auxin signaling and lateral root development in Arabidopsis. Plant J **34:** 67–75

Brocard-Gifford I, Lynch TJ, Garcia ME, Malhotra B, Finkelstein RR (2004) The Arabidopsis thaliana ABSCISIC ACID-INSENSITIVE8 encodes a novel protein mediating abscisic acid and sugar responses essential for growth. Plant Cell **16:** 406–421

Cazzonelli CI, Vanstraelen M, Simon S, Yin K, Carron-Arthur A, Nisar N, Tarle G, Cuttriss AJ, Searle IR, Benkova E, et al (2013) Role of the Arabidopsis PIN6 auxin transporter in auxin homeostasis and auxin-mediated development. PLoS One **8:** e70069

Chen H, Zhang Z, Teng K, Lai J, Zhang Y, Huang Y, Li Y, Liang L, Wang Y, Chu C, et al (2010) Up-regulation of LSB1/GDU3 affects geminivirus infection by activating the salicylic acid pathway. Plant J **62:** 12–23

Chowdary TK, Raman B, Ramakrishna T, Rao ChM (2007) Interaction of mammalian Hsp22 with lipid membranes. Biochem J **401:** 437–445

Cox DN, Muday GK (1994) NPA binding activity is peripheral to the plasma membrane and is associated with the cytoskeleton. Plant Cell **6:** 1941–1953

Cui F, Liu L, Zhao Q, Zhang Z, Li Q, Lin B, Wu Y, Tang S, Xie Q (2012) Arabidopsis ubiquitin conjugase UBC32 is an ERAD component that functions in brassinosteroid-mediated salt stress tolerance. Plant Cell **24:** 233–244

Cutler SR, Rodriguez PL, Finkelstein RR, Abrams SR (2010) Abscisic acid: emergence of a core signaling network. Annu Rev Plant Biol **61:** 651–679

Deak KI, Malamy J (2005) Osmotic regulation of root system architecture. Plant J **43:** 17–28

De Rybel B, Vassileva V, Parizot B, Demeulenaere M, Grunewald W, Audenaert D, Van Campenhout J, Overvoorde P, Jansen L, Vanneste S, et al (2010) A novel aux/IAA28 signaling cascade activates GATA23-dependent specification of lateral root founder cell identity. Curr Biol **20:** 1697–1706

Dharmasiri N, Dharmasiri S, Estelle M (2005) The F-box protein TIR1 is an auxin receptor. Nature **435:** 441–445

Ding Z, Wang B, Moreno I, Dupláková N, Simon S, Carraro N, Reemmer J, Pěnčík A, Chen X, Tejos R, et al (2012) ER-localized auxin transporter PIN8 regulates auxin homeostasis and male gametophyte development in Arabidopsis. Nat Commun **3:** 941

Ding ZJ, Yan JY, Li CX, Li GX, Wu YR, Zheng SJ (2015) Transcription factor WRKY46 modulates the development of Arabidopsis lateral roots in osmotic/salt stress conditions via regulation of ABA signaling and auxin homeostasis. Plant J **84:** 56–69

Engstrom EM, Andersen CM, Gumulak-Smith J, Hu J, Orlova E, Sozzani R, Bowman JL (2011) Arabidopsis homologs of the petunia hairy meristem gene are required for maintenance of shoot and root indeterminacy. Plant Physiol **155:** 735–750

Franklin KA, Lee SH, Patel D, Kumar SV, Spartz AK, Gu C, Ye S, Yu P, Breen G, Cohen JD, et al (2011) Phytochrome-interacting factor 4 (PIF4) regulates auxin biosynthesis at high temperature. Proc Natl Acad Sci USA **108:** 20231–20235

Friml J (2010) Subcellular trafficking of PIN auxin efflux carriers in auxin transport. Eur J Cell Biol **89:** 231–235

Friml J, Vieten A, Sauer M, Weijers D, Schwarz H, Hamann T, Offringa R, Jürgens G (2003) Efflux-dependent auxin gradients establish the apical-basal axis of Arabidopsis. Nature **426:** 147–153

Fukaki H, Tameda S, Masuda H, Tasaka M (2002) Lateral root formation is blocked by a gain-of-function mutation in the *SOLITARY-ROOT/IAA14* gene of Arabidopsis. Plant J **29:** 153–168

Fukaki H, Tasaka M (2009) Hormone interactions during lateral root formation. Plant Mol Biol **69:** 437–449

Geldner N, Anders N, Wolters H, Keicher J, Kornberger W, Muller P, Delbarre A, Ueda T, Nakano A, Jürgens G (2003) The Arabidopsis GNOM ARF-GEF mediates endosomal recycling, auxin transport, and auxin-dependent plant growth. Cell **112:** 219–230

Geldner N, Friml J, Stierhof YD, Jürgens G, Palme K (2001) Auxin transport inhibitors block PIN1 cycling and vesicle trafficking. Nature **413:** 425–428

Gosti F, Beaudoin N, Serizet C, Webb AAR, Vartanian N, Giraudat J (1999) ABI1 protein phosphatase 2C is a negative regulator of abscisic acid signaling. Plant Cell **11:** 1897–1910

Gray WM, Kepinski S, Rouse D, Leyser O, Estelle M (2001) Auxin regulates SCF(TIR1)-dependent degradation of AUX/IAA proteins. Nature **414:** 271–276

Gray WM, Ostin A, Sandberg G, Romano CP, Estelle M (1998) High temperature promotes auxin-mediated hypocotyl elongation in Arabidopsis. Proc Natl Acad Sci USA **95:** 7197–7202

Haslbeck M, Franzmann T, Weinfurtner D, Buchner J (2005) Some like it hot: the structure and function of small heat-shock proteins. Nat Struct Mol Biol **12:** 842–846

He J, Duan Y, Hua D, Fan G, Wang L, Liu Y, Chen Z, Han L, Qu LJ, Gong Z (2012) DEXH box RNA helicase-mediated mitochondrial reactive oxygen species production in Arabidopsis mediates crosstalk between abscisic acid and auxin signaling. Plant Cell **24:** 1815–1833

Helm KW, LaFayette PR, Nagao RT, Key JL, Vierling E (1993) Localization of small heat shock proteins to the higher plant endomembrane system. Mol Cell Biol **13:** 238–247

Helm KW, Schmeits J, Vierling E (1995) An endomembrane-localized small heat-shock protein from *Arabidopsis thaliana*. Plant Physiol **107:** 287–288

Hoth S, Morgante M, Sanchez JP, Hanafey MK, Tingey SV, Chua NH (2002) Genome-wide gene expression profiling in *Arabidopsis thaliana* reveals new targets of abscisic acid and largely impaired gene regulation in the *abi1-1* mutant. J Cell Sci **115:** 4891–4900

Ikeda Y, Men S, Fischer U, Stepanova AN, Alonso JM, Ljung K, Grebe M (2009) Local auxin biosynthesis modulates gradient-directed planar polarity in Arabidopsis. Nat Cell Biol **11:** 731–738

Ito T, Motohashi R, Kuromori T, Mizukado S, Sakurai T, Kanahara H, Seki M, Shinozaki K (2002) A new resource of locally transposed dissociation elements for screening gene-knockout lines in silico on the Arabidopsis genome. Plant Physiol **129:** 1695–1699

Jakob U, Gaestel M, Engel K, Buchner J (1993) Small heat shock proteins are molecular chaperones. J Biol Chem **268:** 1517–1520

Kepinski S, Leyser O (2005) The Arabidopsis F-box protein TIR1 is an auxin receptor. Nature **435:** 446–451

Kim DH, Xu ZY, Na YJ, Yoo YJ, Lee J, Sohn EJ, Hwang I (2011) Small heat shock protein Hsp17.8 functions as an AKR2A cofactor in the targeting of chloroplast outer membrane proteins in Arabidopsis. Plant Physiol **157:** 132–146

Kim DY, Scalf M, Smith LM, Vierstra RD (2013) Advanced proteomic analyses yield a deep catalog of ubiquitylation targets in Arabidopsis. Plant Cell **25:** 1523–1540

Kim KK, Kim R, Kim SH (1998) Crystal structure of a small heat-shock protein. Nature **394:** 595–599

Kleine-Vehn J, Friml J (2008) Polar targeting and endocytic recycling in auxin-dependent plant development. Annu Rev Cell Dev Biol **24:** 447–473

Kuppusamy KT, Walcher CL, Nemhauser JL (2009) Cross-regulatory mechanisms in hormone signaling. Plant Mol Biol **69:** 375–381

Kuromori T, Hirayama T, Kiyosue Y, Takabe H, Mizukado S, Sakurai T, Akiyama K, Kamiya A, Ito T, Shinozaki K (2004) A collection of 11 800 single-copy Ds transposon insertion lines in Arabidopsis. Plant J **37:** 897–905

Lee JS, Wang S, Sritubtim S, Chen JG, Ellis BE (2009) Arabidopsis mitogen-activated protein kinase MPK12 interacts with the MAPK phosphatase IBR5 and regulates auxin signaling. Plant J **57:** 975–985

Liu L, Zhang Y, Tang S, Zhao Q, Zhang Z, Zhang H, Dong L, Guo H, Xie Q (2010) An efficient system to detect protein ubiquitination by agroinfiltration in *Nicotiana benthamiana*. Plant J **61:** 893–903

Liu PP, Montgomery TA, Fahlgren N, Kasschau KD, Nonogaki H, Carrington JC (2007) Repression of AUXIN RESPONSE FACTOR10 by microRNA160 is critical for seed germination and post-germination stages. Plant J **52:** 133–146

MacRae TH (2000) Structure and function of small heat shock/alpha-crystallin proteins: established concepts and emerging ideas. Cell Mol Life Sci **57:** 899–913

Manzano C, Ramirez-Parra E, Casimiro I, Otero S, Desvoyes B, De Rybel B, Beeckman T, Casero P, Gutierrez C, C Del Pozo J, et al (2012) Auxin and epigenetic regulation of SKP2B, an F-box that represses lateral root formation. Plant Physiol **160:** 749–762

Meinhard M, Grill E (2001) Hydrogen peroxide is a regulator of ABI1, a protein phosphatase 2C from Arabidopsis. FEBS Lett **508:** 443–446

Monroe-Augustus M, Zolman BK, Bartel B (2003) IBR5, a dual-specificity phosphatase-like protein modulating auxin and abscisic acid responsiveness in Arabidopsis. Plant Cell **15:** 2979–2991

Mravec J, Skůpa P, Bailly A, Hoyerová K, Krecek P, Bielach A, Petrásek J, Zhang J, Gaykova V, Stierhof YD, et al (2009) Subcellular homeostasis of phytohormone auxin is mediated by the ER-localized PIN5 transporter. Nature **459:** 1136–1140

Nag R, Maity MK, Dasgupta M (2005) Dual DNA binding property of ABA insensitive 3 like factors targeted to promoters responsive to ABA and auxin. Plant Mol Biol **59:** 821–838

Napier RM, Fowke LC, Hawes C, Lewis M, Pelham HRB (1992) Immunological evidence that plants use both HDEL and KDEL for targeting proteins to the endoplasmic reticulum. J Cell Sci **102:** 261–271

Parcellier A, Schmitt E, Gurbuxani S, Seigneurin-Berny D, Pance A, Chantôme A, Plenchette S, Khochbin S, Solary E, Garrido C (2003) HSP27 is a ubiquitin-binding protein involved in I-kappaBalpha proteasomal degradation. Mol Cell Biol **23:** 5790–5802

Parcy F, Giraudat J (1997) Interactions between the ABI1 and the ectopically expressed ABI3 genes in controlling abscisic acid responses in Arabidopsis vegetative tissues. Plant J **11:** 693–702

Petrásek J, Friml J (2009) Auxin transport routes in plant development. Development **136:** 2675–2688

Rinaldi MA, Liu J, Enders TA, Bartel B, Strader LC (2012) A gain-of-function mutation in IAA16 confers reduced responses to auxin and abscisic acid and impedes plant growth and fertility. Plant Mol Biol **79:** 359–373

Rock CD, Sun X (2005) Crosstalk between ABA and auxin signaling pathways in roots of *Arabidopsis thaliana* (L.) Heynh. Planta **222:** 98–106

Ruzicka K, Strader LC, Bailly A, Yang H, Blakeslee J, Langowski L, Nejedlá E, Fujita H, Itoh H, Syono K, et al (2010) Arabidopsis PIS1 encodes the ABCG37 transporter of auxinic compounds including the auxin precursor indole-3-butyric acid. Proc Natl Acad Sci USA **107:** 10749–10753

Saez A, Robert N, Maktabi MH, Schroeder JI, Serrano R, Rodriguez PL (2006) Enhancement of abscisic acid sensitivity and reduction of water consumption in Arabidopsis by combined inactivation of the protein phosphatases type 2C ABI1 and HAB1. Plant Physiol **141:** 1389–1399

Sauer M, Robert S, Kleine-Vehn J (2013) Auxin: simply complicated. J Exp Bot **64:** 2565–2577

Scharf KD, Siddique M, Vierling E (2001) The expanding family of *Arabidopsis thaliana* small heat stress proteins and a new family of proteins containing alpha-crystallin domains (Acd proteins). Cell Stress Chaperones **6:** 225–237

Shinozaki K, Yamaguchi-Shinozaki K (2007) Gene networks involved in drought stress response and tolerance. J Exp Bot **58:** 221–227

Shkolnik-Inbar D, Bar-Zvi D (2010) ABI4 mediates abscisic acid and cytokinin inhibition of lateral root formation by reducing polar auxin transport in Arabidopsis. Plant Cell **22:** 3560–3573

Staswick PE, Serban B, Rowe M, Tiryaki I, Maldonado MT, Maldonado MC, Suza W (2005) Characterization of an Arabidopsis enzyme family that conjugates amino acids to indole-3-acetic acid. Plant Cell **17:** 616–627

Strader LC, Monroe-Augustus M, Bartel B (2008) The IBR5 phosphatase promotes Arabidopsis auxin responses through a novel mechanism distinct from TIR1-mediated repressor degradation. BMC Plant Biol **8:** 41

Sun J, Qi L, Li Y, Chu J, Li C (2012) PIF4-mediated activation of YUCCA8 expression integrates temperature into the auxin pathway in regulating Arabidopsis hypocotyl growth. PLoS Genet **8:** e1002594

Swarup K, Benková E, Swarup R, Casimiro I, Péret B, Yang Y, Parry G, Nielsen E, De Smet I, Vanneste S, et al (2008) The auxin influx carrier LAX3 promotes lateral root emergence. Nat Cell Biol **10:** 946–954

Tanaka H, Dhonukshe P, Brewer PB, Friml J (2006) Spatiotemporal asymmetric auxin distribution: a means to coordinate plant development. Cell Mol Life Sci **63:** 2738–2754

Tatematsu K, Kumagai S, Muto H, Sato A, Watahiki MK, Harper RM, Liscum E, Yamamoto KT (2004) MASSUGU2 encodes Aux/IAA19, an auxin-regulated protein that functions together with the transcriptional activator NPH4/ARF7 to regulate differential growth responses of hypocotyl and formation of lateral roots in *Arabidopsis thaliana*. Plant Cell **16:** 379–393

Tiryaki I, Staswick PE (2002) An Arabidopsis mutant defective in jasmonate response is allelic to the auxin-signaling mutant *axr1*. Plant Physiol **130:** 887–894

Török Z, Goloubinoff P, Horváth I, Tsvetkova NM, Glatz A, Balogh G, Varvasovszki V, Los DA, Vierling E, Crowe JH, et al (2001) Synechocystis HSP17 is an amphitropic protein that stabilizes heat-stressed membranes and binds denatured proteins for subsequent chaperone-mediated refolding. Proc Natl Acad Sci USA **98:** 3098–3103

Ulmasov T, Murfett J, Hagen G, Guilfoyle TJ (1997) Aux/IAA proteins repress expression of reporter genes containing natural and highly active synthetic auxin response elements. Plant Cell **9:** 1963–1971

van Montfort RL, Basha E, Friedrich KL, Slingsby C, Vierling E (2001) Crystal structure and assembly of a eukaryotic small heat shock protein. Nat Struct Biol **8:** 1025–1030

Vanneste S, Friml J (2009) Auxin: a trigger for change in plant development. Cell **136:** 1005–1016

Vanstraelen M, Benková E (2012) Hormonal interactions in the regulation of plant development. Annu Rev Cell Dev Biol **28:** 463–487

Vieten A, Vanneste S, Wisniewska J, Benková E, Benjamins R, Beeckman T, Luschnig C, Friml J (2005) Functional redundancy of PIN proteins is accompanied by auxin-dependent cross-regulation of PIN expression. Development **132:** 4521–4531

Wang L, Hua D, He J, Duan Y, Chen Z, Hong X, Gong Z (2011) Auxin Response Factor2 (ARF2) and its regulated homeodomain gene HB33 mediate abscisic acid response in Arabidopsis. PLoS Genet **7:** e1002172

Waters ER, Lee GJ, Vierling E (1996) Evolution, structure and function of the small heat shock proteins in plants. J Exp Bot **47:** 325–338

Winter D, Vinegar B, Nahal H, Ammar R, Wilson GV, Provart NJ (2007) An "Electronic Fluorescent Pictograph" browser for exploring and analyzing large-scale biological data sets. PLoS One **2:** e718

Wu Y, Li Y, Liu Y, Xie Q (2015) Cautionary notes on the usage of *abi1-2* and *abi1-3* mutants of Arabidopsis ABI1 for functional studies. Mol Plant **8:** 335–338

Zhang H, Jennings A, Barlow PW, Forde BG (1999) Dual pathways for regulation of root branching by nitrate. Proc Natl Acad Sci USA **96:** 6529–6534

Zhang W, Qin C, Zhao J, Wang X (2004) Phospholipase D alpha 1-derived phosphatidic acid interacts with ABI1 phosphatase 2C and regulates abscisic acid signaling. Proc Natl Acad Sci USA **101:** 9508–9513

Zhang X, Henriques R, Lin SS, Niu QW, Chua NH (2006) Agrobacterium-mediated transformation of *Arabidopsis thaliana* using the floral dip method. Nat Protoc **1:** 641–646

Zhang Y, Yang C, Li Y, Zheng N, Chen H, Zhao Q, Gao T, Guo H, Xie Q (2007) SDIR1 is a RING finger E3 ligase that positively regulates stress-responsive abscisic acid signaling in Arabidopsis. Plant Cell **19:** 1912–1929

Zhao C, Shono M, Sun A, Yi S, Li M, Liu J (2007) Constitutive expression of an endoplasmic reticulum small heat shock protein alleviates endoplasmic reticulum stress in transgenic tomato. J Plant Physiol **164:** 835–841

Zhao Y (2010) Auxin biosynthesis and its role in plant development. Annu Rev Plant Biol **61:** 49–64

Zhou W, Wei L, Xu J, Zhai Q, Jiang H, Chen R, Chen Q, Sun J, Chu J, Zhu L, et al (2010) Arabidopsis Tyrosylprotein sulfotransferase acts in the auxin/PLETHORA pathway in regulating postembryonic maintenance of the root stem cell niche. Plant Cell **22:** 3692–3709

Zhu JK (2002) Salt and drought stress signal transduction in plants. Annu Rev Plant Biol **53:** 247–273